

# Common Structure Discovery in Collections of Bipartite Networks: Application to Pollination Systems

Louis Lacoste<sup>1</sup>, Pierre Barbillon<sup>1</sup>, and Sophie Donnet<sup>1</sup>

<sup>1</sup>Université Paris-Saclay, AgroParisTech, INRAE, UMR MIA Paris-Saclay, 91120, Palaiseau, France

## Abstract

Bipartite networks are widely used to encode the ecological interactions. Being able to compare the organization of bipartite networks is a first step toward a better understanding of how environmental factors shape community structure and resilience. Yet current methods for structure detection in bipartite networks overlook shared patterns across collections of networks. We introduce the *colBiSBM*, a family of probabilistic models for collections of bipartite networks that extends the classical Latent Block Model (LBM). The proposed framework assumes that networks are independent realizations of a shared mesoscale structure, encoded through common inter-block connectivity parameters. We establish identifiability conditions for the different variants of *colBiSBM* and develop a variational EM algorithm for parameter estimation, coupled with an adaptation of the integrated classification likelihood (ICL) criterion for model selection. We demonstrate how our approach can be used to classify networks based on their topology or organization. Simulation studies highlight the ability of *colBiSBM* to recover common structures, improve clustering performance, and enhance link prediction by borrowing strength across networks. An application to plant–pollinator networks highlights how the method uncovers shared ecological roles and partitions networks into sub-collections with similar connectivity patterns. These results illustrate the methodological and practical advantages of joint modeling over separate network analyses in the study of bipartite systems.

## 1 Introduction

**Context** Plant–pollinator networks are increasingly documented across the globe (see [Doré et al., 2021](#) and references therein). These systems belong to the broader class of bipartite graphs, which also capture other types of ecological interactions between two sets of actors, such as bird–seed dispersal, prey–predator, or host–parasite relationships ([Kaszewska-Gilas et al., 2021](#); “Web of Life: Ecological Networks Database”, 2022).

Bipartite graphs are widely applied in biology, not only for ecological networks but also in fields such as medicine, where they are used to model biomedical, biomolecular, and epidemiological networks ([Pavlopoulos et al., 2018](#)). Numerous metrics are commonly employed to characterize bipartite networks, including connectivity and nestedness (see [Corso et al., 2011](#)). However, methods for comparing bipartite networks based on their topology remain under active development. Advancing our understanding of bipartite networks and the functional roles of communities is crucial for ecosystem conservation and management ([Elle et al., 2012](#); [Sheykhal et al., 2020](#)).

A flexible and widely used approach for uncovering mesoscale structure in bipartite networks is the Latent Block Model (LBM) ([Govaert and Nadif, 2003, 2010](#)) also known as biSBM (for

bipartite SBM). In this model, each node is associated with a latent variable that assigns it to a functional group or block. Nodes in the same block are assumed to have similar connectivity patterns, so biSBM grouping can reveal functional organization, with potential ecological interpretation. However, the standard biSBM applies to a single network at a time. While one could independently infer biSBMs for each network in a collection and then compare their structures, this approach has clear limitations: in particular, block assignments are not guaranteed to correspond across networks. Being able to compare bipartite networks in ecology would provide an interesting framework to uncover how species interactions shape biodiversity, ecosystem stability, and functional resilience, offering crucial insights for understanding environmental change and guiding conservation efforts. This motivates us to develop a new model for structure detection in collections of bipartite networks.

**Our contribution** We propose to jointly model a collection of bipartite networks by extending the LBM. We assume that the networks are independent realizations of the biSBM, sharing common parameters. From this assumption, an interesting implication is that the groups represent a shared connectivity structure, which can be interpreted as functional groups. Note that we consider networks involving their own nodes, no assumption of correspondence between nodes across networks is made. If some networks involve common individuals (species) then, our approach does not take this information into account and, possibly, the nodes representing the same individual/species across multiple networks may be allocated to different blocks. The proposed model is referred to as the *colBiSBM*, standing for *collection of bipartite stochastic block models*. We introduce several variants of the model, including one where the networks are assumed to be identically distributed according to the same biSBM. Recognizing that this assumption may be overly restrictive for real-world data, we propose an alternative that allows for fluctuations in block proportions, including the possibility of certain blocks being unpopulated. This flexibility enables networks to share only parts of their connectivity structures.

Inference of the parameters, block memberships, and model selection is performed using established tools for SBM and LBM models, building on the work of [Chabert-Liddell et al., 2024](#). Specifically, we employ Variational Expectation-Maximization and an adaptation of the Integrated Classification Likelihood (ICL, [Daudin et al., 2008](#)) for model selection, incorporating novel strategies for model-space exploration.

Three key features of the *colBiSBM* model are particularly noteworthy. First, it enables the identification of a shared connectivity structure that accounts for the observed collection of networks, while also assessing whether this joint modeling approach is appropriate for the collection. By sharing connectivity and, consequently, functional groups, the model facilitates the identification of nodes that exhibit similar ecological roles across different networks. Second, we show how our model can be used to partition the collection of networks thus leading to sub-collections of networks that are similar in terms of their connectivity structures. These two capabilities address critical needs in ecological research, as highlighted by [Michalska-Smith and Allesina, 2019](#); [Pichon et al., 2024](#). Finally, a notable advantage of joint modeling is its ability to transfer information between networks that share a common structure. This approach improves the recovery of more detailed connectivity structures and block memberships, while also facilitating the prediction of missing links ([Clauset et al., 2008](#)) by utilizing connectivity patterns observed throughout the entire collection, thus using mesoscale information instead of local information ([Zhou et al., 2009](#)) to predict missing links.

**Related work** Ecological studies increasingly analyze collections of networks rather than single systems. For example, [Doré et al., 2021](#) investigate anthropogenic pressures across a large dataset of plant–pollinator networks, examining species richness, connectance, and the influence of covariates. Similarly, [Pichon et al., 2024](#) use multi-scale structural descriptors—such as de-

gree distributions, motif frequencies, and nestedness—to differentiate mutualistic and antagonistic networks, identifying structural signatures of interaction types. For pairwise graph comparison, one can rely on dedicated metrics (see [Wills and Meyer, 2020](#)). More recently, graph embedding techniques (see review by [Xu, 2021](#)), often based on neural networks, have become popular: they map graphs into a low-dimensional latent space, making clustering-based comparisons possible. While these approaches are highly scalable, they generally lack the interpretability of block model based methods. Joint modeling of network collections has been studied mostly in the context of unipartite networks. For instance, [Arroyo et al., 2021](#) introduce the *common subspace independent edge* random graph model, which captures a shared invariant subspace across networks. Building on SBM theory, [Agterberg et al., 2025](#) analyse the multilayer degree-corrected stochastic block model (ML-DCSBM), proposing a spectral algorithm that aggregates normalized embeddings across layers. Both approaches assume that nodes are shared across networks in a multilayer collection. In contrast, [Kumpulainen et al., 2024](#) consider collections of SBMs that share a *core* subset of  $s$  blocks, with the remaining blocks being network-specific. Finally, [Matiás and Miele, 2017](#) address temporal network sequences, where the underlying connectivity structure evolves over time.

**Outline** The remainder of this paper is organized as follows. In Section 2.1, we introduce the biSBM for a single bipartite network and apply it independently to a collection of four plant-pollinator networks. Section 3 presents the *colBiSBM* model and its variants. Subsequently, Sections 4.1 and 4.2 provide the likelihood of the models and establish the identifiability of their parameters. In Sections 4.3 and 4.4, we detail the inference strategy (parameter estimation, selection of the numbers of blocks). In Section 4.5, we demonstrate that our method enables the partitioning of a collection of networks into sub-collections sharing a common mesoscopic organization. Finally, in Section 5, we apply our methodology to a collection of five plant-pollinator networks and stress its benefits.

## 2 Data motivation and existing models

### 2.1 Plant-pollinator networks in British cities

Let us consider a collection of  $M$  bipartite networks, each of them representing an (eco)-system involving its own entities. Each bipartite network  $m$  has two sets of nodes of respective sizes  $n_1^m$  and  $n_2^m$ , and the interactions only occur between nodes of set 1 and of set 2. For each network, one can define its bi-adjacency matrix  $(X^m)_{m \in \{1, \dots, M\}}$  of size  $n_1^m \times n_2^m$  such that  $\forall (i, j) \in \llbracket 1, n_1^m \rrbracket \times \llbracket 1, n_2^m \rrbracket$ :

$$\begin{cases} X_{ij}^m = 0 & \text{if no interaction is observed between species } i \text{ and } j \text{ in network } m \\ X_{ij}^m \neq 0 & \text{otherwise.} \end{cases}$$

With this formalism, the nodes of set 1 (e.g., pollinators) are in row and the nodes of set 2 (e.g., plants) are in column. In the following we will talk about row and column nodes. If the network represents binary observations (like presence-absence) then  $X_{ij}^m \in \{0, 1\}$ ; if the interactions are weighted (like an abundance count),  $X_{ij}^m \in \mathbb{N}$ . In what follows, we assume that all the networks in the collection have the same valuation of the interactions. We denote by  $\mathbf{X} = (X^1, \dots, X^M)$  the collection of bi-adjacency matrices.

**Plant-pollinator networks in British cities** We present here a collection of  $M = 4$  plant-pollinator networks from [Baldock et al., 2019](#). This paper studies the diversity, robustness and impact of the type of environment on the ecological aspect of plant-pollinator networks in four

Table 1 – Characteristics of the four British plant-pollinator networks

$m$	Place	nb. of pollinators ( $n_1^m$ )	nb. of plants ( $n_2^m$ )	nb. of $\neq 0$ inter.	density
1	Bristol	180	193	662	0.019
2	Edinburgh	129	137	425	0.024
3	Leeds	126	154	573	0.029
4	Reading	167	156	574	0.022

major British cities, namely Bristol, Edinburgh, Leeds and Reading. The original interactions are abundance counts but, in order to remove potential sampling or species abundance effects, we consider them as binary interactions by setting  $X_{ij}^m = 1$  if pollinator  $i$  has visited plant  $j$  at least once. Their characteristics in terms of number of nodes and density are provided in Table 1. Note that at most 35% of the species (plants or pollinators) are shared by any pair of networks. Additional details on the networks are provided in Table S-3.

We are interested in the global organization of those four networks and not specifically on the role played by each species in its ecosystem. When willing to understand how the networks are organized, the Stochastic Block Model (in short, SBM) has proved its capacity to capture various complex structures, (see [Sander et al., 2015](#) for instance). This model has been extended to bipartite networks resulting into the bipartite Stochastic Block Model (biSBM), also known as the Latent Block Model ([Govaert and Nadif, 2003](#)).

## 2.2 Separate biSBM (sep-biSBM)

The first naive way to deal with multiple networks is to adjust the biSBM separately on each network and then "compare" the resulting structures. The biSBM is a latent variable model, assuming that the row and column nodes of each network  $m$  are divided into respectively  $Q_1^m$  and  $Q_2^m$  blocks. Let  $Z^m = (Z_1^m, \dots, Z_i^m, \dots, Z_{n_1^m}^m)$  and  $W^m = (W_1^m, \dots, W_j^m, \dots, W_{n_2^m}^m)$  encode the belongings of the nodes to their blocks:  $Z_i^m = q$  if row node  $i$  of network  $m$  belongs to row block  $q$  ( $q \in \{1, \dots, Q_1^m\}$ ) and  $W_j^m = r$  if column node  $j$  of network  $m$  belongs to column block  $r$  ( $r \in \{1, \dots, Q_2^m\}$ ). The  $Z_i^m$  and  $W_j^m$  are independent categorical variables with probability:

$$\mathbb{P}(Z_i^m = q) = \pi_q^m, \quad \mathbb{P}(W_j^m = r) = \rho_r^m \quad (1)$$

where  $\pi_q^m > 0$ ,  $\rho_r^m > 0$ ,  $\sum_{q=1}^{Q_1^m} \pi_q^m = 1$  and  $\sum_{r=1}^{Q_2^m} \rho_r^m = 1$ . Given the latent variables  $(Z^m, W^m)$ , the  $X_{ij}^m$ 's are assumed to be independent and distributed as

$$X_{ij}^m \mid Z_i^m = q, W_j^m = r \sim \mathcal{F}(\cdot; \alpha_{qr}^m) \quad (2)$$

where  $\mathcal{F}$  is referred to as the emission distribution.  $\mathcal{F}$  is chosen to be the Bernoulli distribution for binary interactions, and the Poisson distribution for weighted interactions such as counts. Let  $f$  be the density of the emission distribution, then:

$$\log f(X_{ij}^m; \alpha_{qr}^m) = \begin{cases} X_{ij}^m \log(\alpha_{qr}^m) + (1 - X_{ij}^m) \log(1 - \alpha_{qr}^m) & \text{for Bernoulli emission} \\ -\alpha_{qr}^m + X_{ij}^m \log(\alpha_{qr}^m) - \log(X_{ij}^m!) & \text{for Poisson emission} \end{cases} \quad (3)$$

Equations (1), (2) and (3) define the biSBM model, and we will now use a short notation:

$$X^m \sim \mathcal{F}\text{-biSBM}_{n_1^m, n_2^m}(Q_1^m, Q_2^m, \boldsymbol{\pi}^m, \boldsymbol{\rho}^m, \boldsymbol{\alpha}^m) \quad \forall m = 1, \dots, M \quad (\text{sep-biSBM})$$

where  $\mathcal{F}$  encodes the emission distribution,  $n_1^m, n_2^m$  are the numbers of row and column nodes,  $Q_1^m, Q_2^m$  are the numbers of row and column blocks in network  $m$ ,  $\boldsymbol{\pi}^m = (\pi_q^m)_{q=1, \dots, Q_1^m}$

and  $\boldsymbol{\rho}^m = (\rho_r^m)_{r=1,\dots,Q_2^m}$  are the block proportion vectors. The  $Q_1^m \times Q_2^m$  matrix  $\boldsymbol{\alpha}^m = (\alpha_{qr}^m)_{q=1,\dots,Q_1^m, r=1,\dots,Q_2^m}$  contains the connectivity parameters, i.e., the parameters of the emission distribution. In this sep-biSBM model, we suppose that each network  $m$  follows a biSBM with its own parameters  $\boldsymbol{\theta}^m = (\boldsymbol{\pi}^m, \boldsymbol{\rho}^m, \boldsymbol{\alpha}^m)$ . Each model is defined up to label switching of the blocks, as the order of the blocks is completely arbitrary.

For given numbers of blocks  $(Q_1^m, Q_2^m)$ , the parameters  $\boldsymbol{\theta}^m$  can be estimated by a variational version of the EM algorithm. This method is implemented in the R package **sbm** (Chiquet et al., 2024; Leger et al., 2021). The number of blocks  $Q_1^m$  and  $Q_2^m$  can be chosen through the Integrated Classification Likelihood criterion (ICL). Details on the variational EM and ICL will be provided in the following section. The biSBM is an unsupervised clustering method in that the blocks cluster the nodes that “behave the same” in the network. The nodes are assigned to blocks by their maximum posterior probability:

$$\begin{aligned}\widehat{Z}_i^m &= \arg \max_{q=1,\dots,Q_1^m} \mathbb{P}(Z_i^m = q \mid X^m, \widehat{\boldsymbol{\theta}}^m), \\ \widehat{W}_j^m &= \arg \max_{r=1,\dots,Q_2^m} \mathbb{P}(W_j^m = r \mid X^m, \widehat{\boldsymbol{\theta}}^m).\end{aligned}$$

**Application on the plant-pollinator networks** We applied the sep-biSBM model on the four British plant-pollinator networks refereed as Bristol, Edinburgh, Leeds and Reading. We obtain 4 blocks of pollinators for all the networks. The number of blocks of plants is chosen to be 3 in the Bristol, Edinburgh and Reading networks but only 2 in the Leeds network. In Figure 1, the four bi-adjacency matrices are arranged according to the blocks obtained by the inference procedure. For each pair of blocks  $(q, r)$ , the background color of the submatrix is chosen to represent the intensity of the interaction  $\alpha_{qr}^m$ . As previously mentioned, the labels assigned to the blocks are entirely arbitrary. Since we aim at comparing the estimated organisation of the networks, we chose to order the row and column blocks with respect to their marginal density. This choice underscores the nestedness present within the networks (a structural element that is frequently observed in plant-pollinator networks, see e.g., Corso et al., 2011). A quick look at Figure 1 suggests the existence of structural similarities in the four organisations and indicates that a joint modeling approach could be beneficial. In the following, we propose several probabilistic models that assume a connectivity structure shared by all the networks of interest.

### 3 Joint modelisation of multiple bipartite networks

We propose several models adapted to collections of networks. All of them assume that the  $(X^m)_{m=1,\dots,M}$  are independent realizations of a biSBM model.

#### 3.1 A collection of i.i.d. biSBM

This first model assumes that all the networks are independent realizations of the same  $Q_1$ - $Q_2$ -biSBM with identical parameters. The iid-colBiSBM is defined as follows:

$$X^m \sim \mathcal{F}\text{-biSBM}_{n_1^m, n_2^m}(Q_1, Q_2, \boldsymbol{\pi}, \boldsymbol{\rho}, \boldsymbol{\alpha}), \quad \forall m = 1, \dots, M \quad (\text{iid-colBiSBM})$$

where  $\forall (q, r) \pi_q > 0, \rho_r > 0, \sum_{q=1}^{Q_1} \pi_q = \sum_{r=1}^{Q_2} \rho_r = 1$ . This model involves

$$\text{NP}(\text{iid-colBiSBM}) = (Q_1 - 1) + (Q_2 - 1) + Q_1 \times Q_2,$$

parameters, the two first terms corresponding to the row and column block proportions and the third term to connectivity parameters.

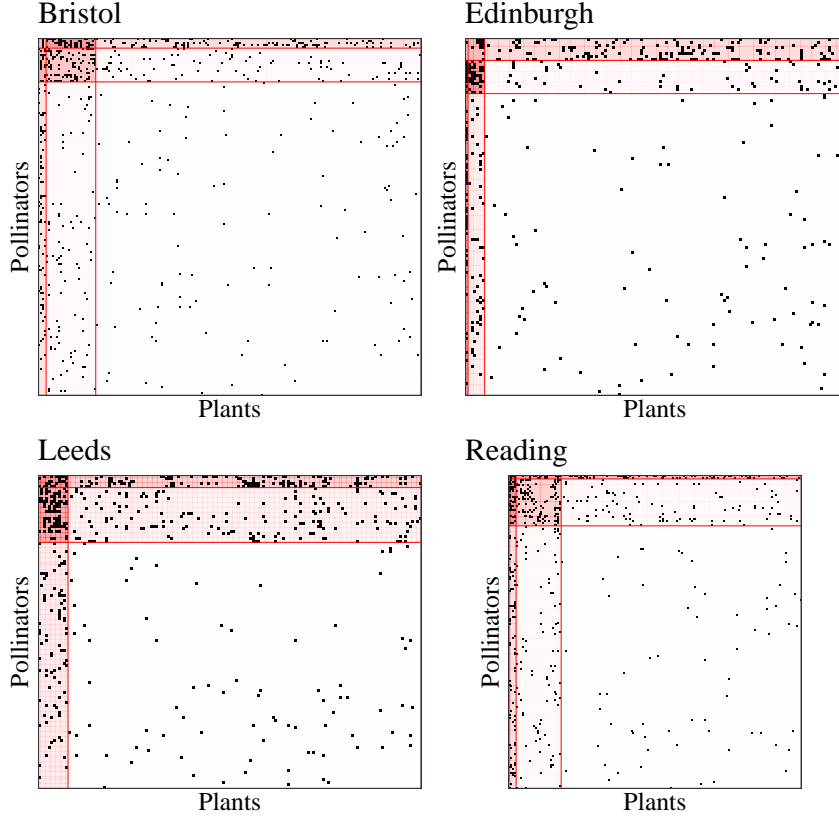


Figure 1 – Matrix representation of the 4 British plant-pollinator networks. The blocks were obtained by fitting a biSBM on each network separately. The blocks were reordered following the marginal probability of connection. The shades of red show the connectivity parameters  $\hat{\alpha}_{qr}^m$ .

By considering the same biSBM model for all the networks, we assume that the systems they represent have a similar global functioning. More interestingly, the inferred blocks in each network will gather species that play the same role across the networks. The role played by each block/cluster in the system is encoded in the unique connectivity matrix  $\alpha$ . However, the iid-colBiSBM also assumes that the block proportions are the same across networks, which means that each block is represented in the same proportion in each network. This is a strong assumption which may not be realistic in plant-pollinator networks and is relaxed in the next section.

### 3.2 A collection of bipartite SBM with varying block size on rows or columns

**$\pi\rho$ -colBiSBM model** Our  $\pi\rho$ -colBiSBM model assumes that the networks share a common connectivity structure represented by  $\alpha$  but that each network has its own row and column block proportions. The  $X^m$  are assumed to be independent and distributed as

$$X^m \sim \mathcal{F}\text{-biSBM}_{n_1^m, n_2^m}(Q_1, Q_2, \pi^m, \rho^m, \alpha), \quad \forall m = 1, \dots, M \quad (\pi\rho\text{-colBiSBM})$$

where  $\forall(q, r)$ ,  $\pi_q^m \geq 0$ ,  $\rho_r^m \geq 0$  and  $\sum_{q=1}^{Q_1} \pi_q^m = \sum_{r=1}^{Q_2} \rho_r^m = 1$ .

This model is more flexible than the iid-colBiSBM as it allows the row block and column block proportions to vary between networks. In addition, we allow some of the  $(\pi_q^m)$ 's and  $(\rho_r^m)$ 's to be null ( $\pi_q^m \in [0, 1]$ ): if  $\pi_q^m = 0$  or  $\rho_r^m = 0$  then the row block  $q$  or column block  $r$  is not represented in the network  $m$ . The connectivity structure of network  $m$  may thus be a subset of a large connectivity structure common to all networks. The possible nullity of some block proportion raises identifiability issues which can be tackled if we assume that each block  $q$  is



represented in at least one network, i.e.,

$$\begin{aligned} \forall q \in \{1, \dots, Q_1\}, \exists m \in \{1, \dots, M\} \text{ such that } \pi_q^m > 0 \\ \forall r \in \{1, \dots, Q_2\}, \exists m \in \{1, \dots, M\} \text{ such that } \rho_r^m > 0 \end{aligned}$$

Let us define the support matrix for row blocks  $S^{(1)}$  of size  $M \times Q_1$  such that  $\forall(m, q)$ ,  $S_{mq}^{(1)} = \mathbb{1}_{\pi_q^m > 0}$ . Then the set of admissible supports is the set of binary matrices with a least one non-null element in each row and column:

$$\mathcal{S}_{Q_1} := \left\{ S^{(1)} \in \mathcal{M}_{M \times Q_1}(\{0, 1\}) \mid \forall m, \sum_{q=1}^{Q_1} S_{mq}^{(1)} > 0, \forall q, \sum_{m=1}^M S_{mq}^{(1)} > 0 \right\}.$$

We define equivalently the support matrix for column blocks  $S^{(2)}$ . For given numbers of blocks  $(Q_1, Q_2)$  and support matrices  $S^{(1)}, S^{(2)}$ , the number of parameters is:

$$\text{NP}(\pi\rho\text{-colBiSBM}) = \sum_{m=1}^M \left( \sum_{q=1}^{Q_1} S_{mq}^{(1)} - 1 \right) + \sum_{m=1}^M \left( \sum_{r=1}^{Q_2} S_{mr}^{(2)} - 1 \right) + \sum_{q,r=1}^{Q_1, Q_2} \mathbb{1}_{(S^{(1)\top} S^{(2)})_{qr} > 0},$$

where  $S^{(1)\top}$  is the transpose of  $S^{(1)}$ . The third quantity takes into account that with  $\pi\rho\text{-colBiSBM}$  some row and column blocks may never interact and thus the corresponding  $\alpha_{qr}$  is not required to define the model.

For the  $\pi\rho\text{-colBiSBM}$  model, we introduce the following notations which will be useful in the next sections.

$$\begin{aligned} \mathcal{Q}_1^m &= \{q \in \{1, \dots, Q_1\} \mid \pi_q^m > 0\}, & Q_1^m &= |\mathcal{Q}_1^m| \\ \mathcal{Q}_2^m &= \{r \in \{1, \dots, Q_2\} \mid \rho_r^m > 0\}, & Q_2^m &= |\mathcal{Q}_2^m| \end{aligned} \quad (4)$$

$Q_1^m$  and  $Q_2^m$  are the numbers of non-empty row and column blocks in network  $m$ .

**$\pi\text{-colBiSBM}$  and  $\rho\text{-colBiSBM}$  models** Some intermediate models can be naturally defined. The  $\pi\text{-colBiSBM}$  allows the row proportions to vary across networks, while keeping the column proportions identical for all networks. The  $\rho\text{-colBiSBM}$  is defined analogously by interchanging rows and columns.

All the models previously defined are summarized in Table 2.

Table 2 – Summary of the different models defined in Section 3. The last line is for separate modelisation as presented in Section 2.

Model name	Row Block prop.	Column Block prop.	Connection param.	Number of param.
iid-colBiSBM	$\pi_q^m = \pi_q, \pi_q > 0$	$\rho_r^m = \rho_r, \rho_r > 0$	$\alpha_{qr}^m = \alpha_{qr}$	$(Q_1 - 1) + (Q_2 - 1) + Q_1 Q_2$
$\pi\text{-colBiSBM}$	$\pi_q^m \geq 0$	$\rho_r^m = \rho_r, \rho_r > 0$	$\alpha_{qr}^m = \alpha_{qr}$	$\leq M(Q_1 - 1) + (Q_2 - 1) + Q_1 Q_2$
$\rho\text{-colBiSBM}$	$\pi_q^m = \pi_q, \pi_q > 0$	$\rho_r^m \geq 0$	$\alpha_{qr}^m = \alpha_{qr}$	$\leq (Q_1 - 1) + M(Q_2 - 1) + Q_1 Q_2$
$\pi\rho\text{-colBiSBM}$	$\pi_q^m \geq 0$	$\rho_r^m \geq 0$	$\alpha_{qr}^m = \alpha_{qr}$	$\leq M(Q_1 - 1) + M(Q_2 - 1) + Q_1 Q_2$
sep-biSBM	$\pi_q^m > 0$	$\rho_r^m > 0$	$\alpha_{qr}^m$	$\sum_{m=1}^M [(Q_1^m - 1) + (Q_2^m - 1) + Q_1^m Q_2^m]$

## 4 Statistical inference

We now address the task of statistical inference. More precisely, we derive the expression of the likelihood, establish the identifiability of the parameters, propose a variational version of the EM algorithm to estimate the parameters, and finally suggest a penalized likelihood criterion to infer the number of blocks. The results and methods are given for  $\pi\rho$ -colBiSBM. The corresponding formula for  $\pi$ -colBiSBM and  $\rho$ -colBiSBM are left to the reader.

### 4.1 Log-likelihood expression for $\pi\rho$ -colBiSBM

For the given matrices  $S^{(1)}, S^{(2)}$ , let  $\boldsymbol{\theta}_{S^{(1)}, S^{(2)}}$  be:

$$\boldsymbol{\theta}_{S^{(1)}, S^{(2)}} = (\boldsymbol{\pi}^1, \dots, \boldsymbol{\pi}^M, \boldsymbol{\rho}^1, \dots, \boldsymbol{\rho}^M, \boldsymbol{\alpha}) = (\boldsymbol{\pi}, \boldsymbol{\rho}, \boldsymbol{\alpha})$$

where  $\pi_q^m = 0$  for any  $q$  such that  $S_{mq}^{(1)} = 0$  and  $\rho_r^m = 0$  for any  $r$  such that  $S_{mr}^{(2)} = 0$ .  $\pi\rho$ -colBiSBM is a latent variable model and consequently, the observed log-likelihood  $\ell(\mathbf{X}; \boldsymbol{\theta}_{S^{(1)}, S^{(2)}})$  is written as the complete likelihood integrated over the latent variables.

Let  $Z^m = (Z_i^m)_{i=1, \dots, n_1^m}$  denote the set a latent variables encoding the clustering of the row nodes in network  $m$ . Similarly, we define and  $W^m = (W_j^m)_{j=1, \dots, n_2^m}$ . The log-likelihood of the observations  $\mathbf{X} = (X^1, \dots, X^M)$  is written as the complete likelihood integrated over the latent variables  $(\mathbf{Z}, \mathbf{W}) = (Z^m, W^m)_{m=1, \dots, M}$ :

$$\ell(\mathbf{X}; \boldsymbol{\theta}_{S^{(1)}, S^{(2)}}) = \sum_{m=1}^M \log \sum_{Z^m, W^m} \exp\{\ell(X^m | Z^m, W^m; \boldsymbol{\alpha}) + \ell(Z^m; \boldsymbol{\pi}) + \ell(W^m; \boldsymbol{\rho})\} \quad (5)$$

where

$$\begin{aligned} \ell(X^m | Z^m, W^m; \boldsymbol{\alpha}) &= \sum_{i=1}^{n_1^m} \sum_{j=1}^{n_2^m} \sum_{q \in \mathcal{Q}_1^m} \sum_{r \in \mathcal{Q}_2^m} \mathbb{1}_{Z_i^m=q, W_j^m=r} \log f(X_{ij}^m; \alpha_{qr}), \\ \ell(Z^m; \boldsymbol{\pi}) &= \sum_{i=1}^{n_1^m} \sum_{q \in \mathcal{Q}_1^m} \mathbb{1}_{Z_i^m=q} \log \pi_q^m, \text{ and } \ell(W^m; \boldsymbol{\rho}) = \sum_{j=1}^{n_2^m} \sum_{r \in \mathcal{Q}_2^m} \mathbb{1}_{W_j^m=r} \log \rho_r^m. \end{aligned}$$

where  $f$  is defined in Equation (3). We obtain the log-likelihood of the iid-colBiSBM model by setting  $\boldsymbol{\pi}^m = \boldsymbol{\pi}$  and  $\boldsymbol{\rho}^m = \boldsymbol{\rho}, \forall m$ ,  $\mathcal{Q}_1^m = \{1, \dots, Q_1\}$  and  $\mathcal{Q}_2^m = \{1, \dots, Q_2\}$ . For the  $\pi$ -colBiSBM and  $\rho$ -colBiSBM models we obtain the log-likelihood by fixing either the row or column proportions, and by setting the relevant support matrix to the matrix full of ones.

### 4.2 Identifiability of the models

We prove the identifiability of the parameters, namely that if  $\ell(\mathbf{X}; \boldsymbol{\theta}) = \ell(\mathbf{X}; \boldsymbol{\theta}')$  for any collection  $\mathbf{X}$  then  $\boldsymbol{\theta} = \boldsymbol{\theta}'$ . The identifiability of the parameters of the simple biSBM is demonstrated in [Keribin et al., 2015](#) as an extension of the result of [Celisse et al., 2012](#). [Chabert-Liddell et al., 2024](#) gave identifiability conditions for collections of simple (non bipartite) networks. We provide here conditions which ensure the identifiability of the model. Note that the conditions are sufficient but not necessary.

In  $\pi\rho$ -colBiSBM, we allow the block proportions to be null in certain networks. Let us first define the restricted parameters for each network, corresponding to the non-null block proportions:

$$\begin{aligned} \overline{\boldsymbol{\pi}}^m &= (\pi_q^m)_{q \in \mathcal{Q}_1^m}, & \overline{\boldsymbol{\rho}}^m &= (\rho_r^m)_{r \in \mathcal{Q}_2^m} \\ \overline{\boldsymbol{\alpha}}^m &= (\alpha_{qr})_{q \in \mathcal{Q}_1^m, r \in \mathcal{Q}_2^m} \end{aligned}$$



**Property 1.** *The parameters  $\boldsymbol{\theta} = (\boldsymbol{\pi}, \boldsymbol{\rho}, \boldsymbol{\alpha})$  of the iid-colBiSBM model are identifiable up to a label switching of the blocks under the following conditions:*

$$(1.1) \exists m^* \in \{1, \dots, M\} : n_1^{m^*} \geq 2Q_2 - 1 \text{ and } n_2^{m^*} \geq 2Q_1 - 1.$$

(1.2) *The coordinates of vector  $\boldsymbol{\alpha}\boldsymbol{\rho}$  are distinct.*

(1.3) *The coordinates of vector  $\boldsymbol{\pi}^\top \boldsymbol{\alpha}$  (where  $\boldsymbol{\pi}^\top$  is the transpose of  $\boldsymbol{\pi}$ ) are distinct.*

*The parameters  $\boldsymbol{\theta}_{S^{(1)}, S^{(2)}} = (\boldsymbol{\pi}^1, \dots, \boldsymbol{\pi}^M, \boldsymbol{\rho}^1, \dots, \boldsymbol{\rho}^M, \boldsymbol{\alpha})$  of the  $\pi\rho$ -colBiSBM are identifiable up to a label switching of the blocks if the following conditions are met:*

$$(2.1) \forall m \in \{1, \dots, M\} : n_1^m \geq 2Q_2^m - 1 \text{ and } n_2^m \geq 2Q_1^m - 1$$

(2.2)  *$\forall m \in \{1, \dots, M\}$ , the coordinates of the vector  $\bar{\boldsymbol{\alpha}}^m \bar{\boldsymbol{\rho}}^m$  are distinct.*

(2.3)  *$\forall m \in \{1, \dots, M\}$ , the coordinates of the vector  $(\bar{\boldsymbol{\pi}}^m)^\top \bar{\boldsymbol{\alpha}}^m$  are distinct.*

(2.4) *All entries of  $\boldsymbol{\alpha}$  are unique.*

The proof is provided in Section A.

### 4.3 Variational estimation of the parameters

We aim to estimate  $\boldsymbol{\theta}_{S^{(1)}, S^{(2)}}$  by maximizing the log-likelihood of Equation (5) for fixed numbers of blocks  $(Q_1, Q_2)$  and fixed support matrices  $(S^{(1)}, S^{(2)})$  in the case of the  $\pi\rho$ -colBiSBM model. However, in practice, this log-likelihood is not tractable as it requires to sum over  $\sum_{m=1}^M (Q_1^m)^{n_1^m} (Q_2^m)^{n_2^m}$  terms. A reliable method to tackle this problem is to rely on a variational version of the Expectation Maximization (VEM) algorithm (Daudin et al., 2008; Govaert and Nadif, 2008).

The maximization of the log-likelihood is replaced by the maximization of a variational lower bound of the log-likelihood of the observed data. For ease of reading, the indices of  $\boldsymbol{\theta}_{S^{(1)}, S^{(2)}}$  are dropped and we use the short notation  $\boldsymbol{\theta}$ . Let  $\mathcal{R}$  be an approximation of  $p(\mathbf{Z}, \mathbf{W} | \mathbf{X}; \boldsymbol{\theta})$ . Then:

$$\begin{aligned} \ell(\mathbf{X}; \boldsymbol{\theta}) &\geq \ell(\mathbf{X}; \boldsymbol{\theta}) - D_{\text{KL}}(\mathcal{R} \parallel p(\mathbf{Z}, \mathbf{W} | \mathbf{X}; \boldsymbol{\theta})) \\ &= \mathbb{E}_{\mathcal{R}}[\ell(\mathbf{X}, \mathbf{Z}, \mathbf{W}; \boldsymbol{\theta})] - \mathcal{H}(\mathcal{R}(\mathbf{Z}, \mathbf{W})) \\ &=: \mathcal{J}(\mathcal{R}; \boldsymbol{\theta}) \end{aligned} \tag{6}$$

where  $D_{\text{KL}}$  is the Kullback-Leibler divergence and  $\mathcal{H}$  is the entropy.  $\mathcal{J}(\mathcal{R}; \boldsymbol{\theta})$  is known as the evidence lower bound (ELBO). Note that  $\mathcal{J}(\mathcal{R}; \boldsymbol{\theta}) = \ell(\mathbf{X}; \boldsymbol{\theta})$  if  $\mathcal{R} = p(\mathbf{Z}, \mathbf{W} | \mathbf{X}; \boldsymbol{\theta})$ . So, the objective is now to maximize  $\mathcal{J}(\mathcal{R}; \boldsymbol{\theta})$  with respect to  $\boldsymbol{\theta}$  and  $\mathcal{R}$ . This task can be performed thanks to the reformulation of the lower bound provided in Equation (6). The VEM algorithm is an iterative process aimed at maximizing the lower bound, that alternates between the E-step and the M-step. During the E-step  $\mathcal{J}(\mathcal{R}; \boldsymbol{\theta})$  is maximized w.r.t.  $\mathcal{R}$  and for a current value of  $\boldsymbol{\theta}$ , resulting into a minimization of  $D_{\text{KL}}(\mathcal{R} \parallel p(\mathbf{Z}, \mathbf{W} | \mathbf{X}; \boldsymbol{\theta}))$ , which can not be performed directly. The M-step maximizes  $\mathcal{J}(\mathcal{R}; \boldsymbol{\theta})$  w.r.t.  $\boldsymbol{\theta}$  for a given variational distribution  $\mathcal{R}$ .  $\mathcal{R}$  must be chosen so that the quantity  $\mathbb{E}_{\mathcal{R}}[\ell(\mathbf{X}, \mathbf{Z}, \mathbf{W}; \boldsymbol{\theta})]$  can be calculated explicitly. By conditional independence of the row and column latent variables given the observations and by independence of the networks we have:

$$\begin{aligned} p(\mathbf{Z}, \mathbf{W} | \mathbf{X}; \boldsymbol{\theta}) &= p(\mathbf{Z} | \mathbf{X}; \boldsymbol{\theta}) p(\mathbf{W} | \mathbf{X}; \boldsymbol{\theta}) \\ &= \prod_{m=1}^M p(\mathbf{Z}^m | \mathbf{X}^m; \boldsymbol{\theta}) p(\mathbf{W}^m | \mathbf{X}^m; \boldsymbol{\theta}). \end{aligned}$$

$\mathcal{R}(\mathbf{Z}, \mathbf{W})$  is assumed to respect the same independence structure. Moreover, following [Daudin et al., 2008; Govaert and Nadif, 2008](#),  $\mathcal{R}(\mathbf{Z})$  and  $\mathcal{R}(\mathbf{W})$  are chosen as product distributions, thus neglecting the conditional dependencies between nodes of a given network. Thus,  $p(Z^m|X^m; \theta)$  is approximated by  $\mathcal{R}(Z^m) = \prod_{i=1}^{n_1^m} p_{\mathcal{R}}(Z_i^m)$  which is parametrized by the probabilities  $\tau_{iq}^{1,m}$ .

$$\tau_{iq}^{1,m} = \mathbb{P}_{\mathcal{R}}(Z_i^m = q).$$

The same holds for  $p(W^m|X^m; \theta)$  and we set:

$$\tau_{jr}^{2,m} = \mathbb{P}_{\mathcal{R}}(W_j^m = r).$$

These quantities are the approximations of the posterior node clustering probabilities. In the following we identify  $\mathcal{R}$  to these quantities.

For the colBiSBM models, the VE-step is computed independently for each network and during the M-step the parameters are updated with formulas that link the networks together.

We describe below the update procedure to go from step  $t$  to  $t+1$ , in our implementation this is done until convergence and we use a mini-batching approach as it converges quicker in the experiments. To initialize the algorithm one can do a spectral clustering of the nodes to determine the first posterior node clustering probabilities.

**Variational E step** At this step we maximize with respect to the variational distribution  $\mathcal{R}$ :

$$\hat{\mathcal{R}}^{(t+1)} = \arg \max_{\mathcal{R}} \mathcal{J}(\mathcal{R}, \hat{\theta}^{(t)}).$$

And we obtain the following formulas for the  $\tau^m = ((\tau_{iq}^{1,m})_{i=1, \dots, n_1^m}, (\tau_{jr}^{2,m})_{j=1, \dots, n_2^m})$ :

$$\begin{cases} \hat{\tau}_{iq}^{1,m} \propto \hat{\pi}_q^{m,(t)} \prod_{j=1}^{n_2^m} \prod_{r \in \mathcal{Q}_2^m} f(X_{ij}^m; \hat{\alpha}_{qr}^{(t)}) \hat{\tau}_{jr}^{2,m,(t+1)} & \forall i = 1, \dots, n_1^m, q \in \mathcal{Q}_1^m \\ \hat{\tau}_{jr}^{2,m} \propto \hat{\rho}_r^{m,(t)} \prod_{i=1}^{n_1^m} \prod_{q \in \mathcal{Q}_1^m} f(X_{ij}^m; \hat{\alpha}_{qr}^{(t)}) \hat{\tau}_{iq}^{1,m,(t+1)} & \forall j = 1, \dots, n_2^m, r \in \mathcal{Q}_2^m \end{cases}$$

which are used to update iteratively the values.

**M step** At iteration  $(t)$  the M-step maximizes the variational bound with respect to the model parameters  $\theta$ :

$$\hat{\theta}^{(t+1)} = \arg \max_{\theta} \mathcal{J}(\hat{\mathcal{R}}^{(t+1)}, \theta)$$

The following quantities are involved in the obtained formulas:

$$e_{qr}^m = \sum_{i=1}^{n_1^m} \sum_{j=1}^{n_2^m} \tau_{iq}^{1,m} \tau_{jr}^{2,m} X_{ij}^m, \quad n_{qr}^m = \sum_{i=1}^{n_1^m} \sum_{j=1}^{n_2^m} \tau_{iq}^{1,m} \tau_{jr}^{2,m}, \quad n_q^{1,m} = \sum_{i=1}^{n_1^m} \tau_{iq}^{1,m}, \quad n_r^{2,m} = \sum_{j=1}^{n_2^m} \tau_{jr}^{2,m}$$

The block proportions estimations depend on the model we consider,

$$\begin{aligned} \hat{\pi}_q &= \frac{\sum_{m=1}^M n_q^{1,m}}{\sum_{m=1}^M n_1^m}, & \hat{\rho}_r &= \frac{\sum_{m=1}^M n_r^{2,m}}{\sum_{m=1}^M n_2^m} & \text{for iid-colBiSBM} \\ \hat{\pi}_q^m &= \frac{n_q^{1,m}}{n_1^m}, & \hat{\rho}_r^m &= \frac{n_r^{2,m}}{n_2^m} & \text{for } \pi\rho\text{-colBiSBM.} \end{aligned}$$

while the connectivity parameters  $\alpha_{qr}$  are estimated as the ratio of the number of observed interactions between row block  $q$  and column block  $r$  among all networks over the number of possible interactions:

$$\hat{\alpha}_{qr} = \frac{\sum_{m=1}^M e_{qr}^m}{\sum_{m=1}^M n_{qr}^m}.$$

**Output of the algorithm** The inference algorithm supplies for each node of any network its probability of clustering given its connections namely the  $\hat{\tau}_{iq}^{1,m}$  and  $\hat{\tau}_{jr}^{2,m}$ . These quantities can be used to perform hard clustering (taking the *maximum a posteriori*, in short, MAP) and so to reorganize the bi-adjacency matrices. Note that contrarily to sep-biSBM (Section 2), the clustering we obtain here are coherent across the networks. In other words, two species from networks  $m$  and  $m'$  affected to a given cluster  $q$  do play the same role in their respective ecosystem. On the contrary, from the ecological point of view, one can check if a given species represented by two different nodes in networks  $m$  and  $m'$  is affected to the same block or plays a different role in the two ecosystems.

#### 4.4 Selecting the numbers of blocks $(Q_1, Q_2)$

Section 4.3 was dedicated to the estimation of  $\theta$  for fixed  $(Q_1, Q_2)$ . In practice the numbers of blocks need to be inferred. We propose a penalized likelihood criterion. We first consider the iid-colBiSBM and then the  $\pi\rho$ -colBiSBM which requires a few more work due to the possibly null block proportions in some of the networks.

##### 4.4.1 A penalized criterion adapted to collections of networks

The Integrated Classification Likelihood (ICL), introduced by [Biernacki et al., 2000](#); [Daudin et al., 2008](#), is a well-established tool for selecting the appropriate number of blocks of SBM and biSBM. The ICL is derived from an asymptotic approximation of the marginal complete likelihood where the parameters are integrated out using a prior distribution, resulting in a penalized likelihood criterion. Usage has shown good recovery properties for the number of blocks. The generic expression of the ICL is

$$\text{ICL} = \max_{\theta} \mathbb{E}_{\hat{\mathcal{R}}}[\ell(\mathbf{X}, \mathbf{Z}, \mathbf{W}; \theta)] - \frac{1}{2}\text{pen}$$

where pen penalizes the complexity of the model. ICL is known to encourage well-separated blocks by imposing a penalty on the entropy of node grouping. However, the objective of our approach extends beyond grouping nodes into coherent blocks. We also aim to assess the similarity of connectivity patterns across different networks. Consequently, we suggest to permit models that offer more flexible node grouping by not penalizing on entropy. This leads us to formulate a BIC-like criterion in the following manner:

$$\text{BIC-L} = \max_{\theta} \mathbb{E}_{\hat{\mathcal{R}}}[\ell(\mathbf{X}, \mathbf{Z}, \mathbf{W}; \theta)] + \mathcal{H}(\hat{\mathcal{R}}) - \frac{1}{2}\text{pen} = \max_{\theta} \mathcal{J}(\hat{\mathcal{R}}, \theta) - \frac{1}{2}\text{pen}$$

We provide below the penalty expressions for iid-colBiSBM and  $\pi\rho$ -colBiSBM.

##### 4.4.2 Model selection for iid-colBiSBM

For iid-colBiSBM, the penalty follows from the same logic as for the classical biSBM since the networks are independent realizations of the same biSBM:

$$\text{BIC-L}(\mathbf{X}, Q_1, Q_2) = \max_{\theta} \mathcal{J}(\hat{\mathcal{R}}, \theta) - \frac{1}{2}[\text{pen}_{\pi}(Q_1) + \text{pen}_{\rho}(Q_2) + \text{pen}_{\alpha}(Q_1, Q_2)]$$

with

$$\begin{aligned} \text{pen}_{\pi}(Q_1) &= (Q_1 - 1) \log \left( \sum_{m=1}^M n_1^m \right), & \text{pen}_{\rho}(Q_2) &= (Q_2 - 1) \log \left( \sum_{m=1}^M n_2^m \right), \\ \text{pen}_{\alpha}(Q_1, Q_2) &= Q_1 Q_2 \log(N_M), \end{aligned}$$

where

$$N_M = \sum_{m=1}^M n_1^m n_2^m, \quad (7)$$

is the number of entries in all the bi-adjacency matrices. The terms  $\text{pen}_\pi(Q_1)$  and  $\text{pen}_\rho(Q_2)$  correspond to the estimation of the block proportions. The term  $\text{pen}_\alpha(Q_1, Q_2)$  is the penalty for the connectivity. And finally  $Q_1$  and  $Q_2$  are chosen as:

$$(\widehat{Q}_1, \widehat{Q}_2) = \arg \max_{Q_1, Q_2} \text{BIC-L}(\mathbf{X}, Q_1, Q_2).$$

#### 4.4.3 Model selection for $\pi\rho\text{-colBiSBM}$

In model  $\pi\rho\text{-colBiSBM}$ , we need to choose not only  $(Q_1, Q_2)$  but also the support matrices  $(S^{(1)}, S^{(2)})$ . The penalty term must take into account the dimension of the supports  $(S^{(1)}, S^{(2)})$  which is the number of non-null proportions namely  $Q_1^m$  and  $Q_2^m$  defined in Equation (4). Considering the same principle as ICL described before, the penalty derives from a prior distribution on  $(S^{(1)}, S^{(2)})$ : a uniform prior over  $\{1, \dots, Q_1\} \times \{1, \dots, Q_2\}$  is set as a prior on  $(Q_1^m, Q_2^m)$ ; then conditionally to  $(Q_1^m, Q_2^m)$ , the place of the non-empty blocks in network  $m$  (i.e.,  $(S_{mq}^{(1)})_{q=1, \dots, Q_1}$  and  $(S_{mr}^{(2)})_{r=1, \dots, Q_2}$ ) are uniformly distributed, resulting into a penalty of the form

$$\log p_{Q_1}(S^{(1)}) = -M \log(Q_1) - \sum_{m=1}^M \log \binom{Q_1}{Q_1^m}$$

where  $\binom{Q_1}{Q_1^m}$  is the number of ways to place the  $Q_1^m$  non empty blocks among the  $Q_1$  possible blocks. The same formula holds for  $p_{Q_2}(S^{(2)})$ . Using the Laplace approximation and the prior distributions we obtain the following criterion:

$$\text{BIC-L}(\mathbf{X}, Q_1, Q_2) = \max_{S^{(1)}, S^{(2)}} \left[ \max_{\theta_{S^{(1)}, S^{(2)}}} \mathcal{J}(\hat{\mathcal{R}}, \theta_{S^{(1)}, S^{(2)}}) - \frac{\text{pen}(Q_1, Q_2, S^{(1)}, S^{(2)}, \alpha, \pi, \rho)}{2} \right].$$

The penalty is composed of the following terms:

$$\text{pen}_\pi(Q_1, S^{(1)}) + \text{pen}_\rho(Q_2, S^{(2)}) + \text{pen}_\alpha(Q_1, Q_2, S^{(1)}, S^{(2)}) + \text{pen}_{S^{(1)}}(Q_1) + \text{pen}_{S^{(2)}}(Q_2),$$

with

$$\text{pen}_{S^{(1)}}(Q_1) = -2 \log p_{Q_1}(S^{(1)}), \quad \text{pen}_{S^{(2)}}(Q_2) = -2 \log p_{Q_2}(S^{(2)}),$$

$$\text{pen}_\pi(Q_1, S^{(1)}) = \sum_{m=1}^M (Q_1^m - 1) \log n_1^m, \quad \text{pen}_\rho(Q_2, S^{(2)}) = \sum_{m=1}^M (Q_2^m - 1) \log n_2^m,$$

and

$$\text{pen}_\alpha(Q_1, Q_2, S^{(1)}, S^{(2)}) = \left( \sum_{q=1}^{Q_1} \sum_{r=1}^{Q_2} \mathbb{1}_{((S^{(1)})', S^{(2)})_{qr} > 0} \right) \log(N_M),$$

where  $N_M$  is defined in Equation (7).  $(Q_1, Q_2)$  are finally chosen by maximizing the BIC-L criterion:

$$(\widehat{Q}_1, \widehat{Q}_2) = \arg \max_{Q_1, Q_2} \text{BIC-L}(\mathbf{X}, Q_1, Q_2).$$

#### 4.4.4 Practical model selection

The choice of  $(Q_1, Q_2)$  and the estimation of the model parameters are computationally expensive. All the models with possible values of  $(Q_1, Q_2)$  should be fitted and compared through the  $\text{BIC-L}(\mathbf{X}, Q_1, Q_2)$  criterion. In addition, for a fixed value of  $(Q_1, Q_2)$ , the variational EM being sensitive to the initialization, multiple runs are needed.

We propose a partial exploration of the model space by a split and merge approach. The first step is a greedy exploration to find an estimation of the mode of the criterion. The second step is a moving window centered around the first mode to refine the first estimation by leveraging all the previously fitted models. The procedure, detailed in Algorithm 1 is implemented in the R-package `colSBM`.

---

##### Algorithm 1: Model selection algorithm

---

**Data:**  $\mathbf{X}$  a collection of bipartite networks  
**Tuning parameters:**  $\max_{\text{ge}}$ ,  $\max_{\text{mw}}$  and  $\text{depth}$   
**begin**  
  | - Fit colBiSBM model with  $\mathbf{Q} = (1, 2)$  and  $\mathbf{Q} = (2, 1)$   
**end**  
   $\text{step}_{\text{ge}} \leftarrow 0$   
  **for**  $\mathbf{Q}_{\text{curr}} \in \{(1, 2), (2, 1)\}$  **do**  
    **while** BIC-L increases and  $\text{step}_{\text{ge}} \leq \max_{\text{ge}}$  ;  $\triangleleft$  Greedy exploration  
    **do**  
      | - Fit the models for  $\mathbf{Q} \in \mathbf{Q}_{\text{curr}} + \{(1, 0), (0, 1)\}$  ;  $\triangleleft$  Splits  
      **if**  $\mathbf{Q}_{\text{curr}}$  allows to merge **then**  
        | - Fit the models for  $\mathbf{Q} \in \mathbf{Q}_{\text{curr}} - \{(1, 0), (0, 1)\}$  ;  $\triangleleft$  Merges  
      **end**  
      -  $\mathbf{Q}_{\text{curr}} \leftarrow \arg \max \text{BIC-L}(\mathbf{X}, Q_1, Q_2)$  and  $\text{step}_{\text{ge}} \leftarrow \text{step}_{\text{ge}} + 1$   
    **end**  
  **end**  
  -  $\mathbf{Q}_{\text{ge}} \leftarrow \mathbf{Q}_{\text{curr}}$  and  $\text{step}_{\text{mw}} \leftarrow 0$   
  **while** BIC-L increases and  $\text{step}_{\text{mw}} \leq \max_{\text{mw}}$  ;  $\triangleleft$  Moving window  
  **do**  
    **for**  $\mathbf{Q}_{\text{curr}} = \mathbf{Q}_{\text{curr}} - \text{depth}, \dots, \mathbf{Q}_{\text{curr}} + \text{depth}$ ;  $\triangleleft$  Forward pass  
    **do**  
      | - Fit the models by splitting from  $\mathbf{Q}_{\text{curr}}$   
    **end**  
    **for**  $\mathbf{Q}_{\text{curr}} = \mathbf{Q}_{\text{curr}} + \text{depth}, \dots, \mathbf{Q}_{\text{curr}} - \text{depth}$ ;  $\triangleleft$  Backward pass  
    **do**  
      | - Fit the models by merging from  $\mathbf{Q}_{\text{curr}}$   
    **end**  
    -  $\mathbf{Q}_{\text{curr}} \leftarrow \arg \max \text{BIC-L}(\mathbf{X}, Q_1, Q_2)$  and  $\text{step}_{\text{mw}} \leftarrow \text{step}_{\text{mw}} + 1$   
  **end**  
**return**  $\widehat{Q}_1, \widehat{Q}_2 = \arg \max \text{BIC-L}(\mathbf{X}, Q_1, Q_2)$  with  $\widehat{\theta}, \widehat{\mathbf{Z}}, \widehat{\mathbf{W}}$  and  $\widehat{S}^{(1)}, \widehat{S}^{(2)}$  for  $\pi\rho\text{-colBiSBM}$  models.

---

## 4.5 Searching for common connectivity structures among a collection of networks

**sep-biSBM versus colBiSBM** Beyond determining the optimal number of blocks, the BIC-L criterion we derived can also be used to test whether two or more bipartite networks share a

common mesoscopic structure. To do so, the first model comparison that we may perform is between the colBiSBM models and the sep-biSBM model to determine if the networks share a common structure. We decide that networks share a common structure if:

$$\max_{Q_1, Q_2} \text{BIC-L}_{\text{colBiSBM}}(\mathbf{X}, Q_1, Q_2) > \sum_{m=1}^M \max_{Q_1^m, Q_2^m} \text{BIC-L}_{\text{biSBM}}(\mathbf{X}^m, Q_1^m, Q_2^m).$$

**Partition of a collection of networks** At a more advanced stage, when considering a large collection of networks as the one described in Doré et al., 2021, one may seek to identify subgroups of networks exhibiting similar connectivity patterns. In other words, the goal is to perform a network partitioning procedure based on their mesoscopic structure i.e., find  $\mathcal{G} = (\mathcal{M}_g)_{g=1, \dots, G}$  a partition of  $\{1, \dots, M\}$  such that

$$\forall m \in \mathcal{M}_g, X^m \sim \mathcal{F}\text{-biSBM}(Q_1^g, Q_2^g, \boldsymbol{\pi}^m, \boldsymbol{\rho}^m, \boldsymbol{\alpha}^g),$$

where  $\boldsymbol{\alpha}^g$  depends on the group the network belongs to. For any partition  $\mathcal{G}$ , we define an adequacy score, denoted by  $Sc(\mathcal{G})$ , which quantifies the fit of the partition according to the BIC-L criterion:

$$Sc(\mathcal{G}) = \sum_{g=1}^G \max_{Q_1^g, Q_2^g} \text{BIC-L}((X^m)_{m \in \mathcal{M}_g}, Q_1^g, Q_2^g) \quad (8)$$

Thus the score consists of the sum of the BIC-L computed on the sub-collections for the partition  $\mathcal{G}$ .  $B_M$  (Bell number) possible partitions have to be compared though this score. If  $M$  is small, the scores of the  $B_M$  possible partitions can be computed by fitting a colSBM to any of the  $2^M$  subcollections of networks. However, if  $M$  is large, this strategy is not realistic anymore for computational considerations. In this case, one can resort to a hierarchical research strategy. In a few words, adjust a unique model on the full collection and then proceed by sequential divisions of the partition based on dissimilarities between parameters. Denoting  $\mathcal{G}^*$  the new partition obtained from  $\mathcal{G}$ , if  $Sc(\mathcal{G}^*) > Sc(\mathcal{G})$  try to partition further, else stop and return  $\mathcal{G}$ . For extensive details see Section C.

## 4.6 Accuracy of the inference strategy on synthetic datasets

We illustrate the accuracy of our inference method on synthetic datasets. The results of our extensive simulation study is available in supplementary material. In Section D.1, we prove the capacity of our inference procedure to recover the number of blocks. The corresponding nodes clustering is assessed under the different colBiSBMs. The ability to choose the correct colBiSBM (through BIC-L) is tested in Section D.2. The interest of a joint learning under a colBiSBM compared to fitting separated biSBMs is demonstrated in Section D.3. Finally, the efficiency of the partitioning procedure of a collection of networks is investigated in Section D.4. All these simulations are reproducible, the code is available at <https://github.com/Polarolouis/code-colbisbm/>.

## 5 Analyzing real-world ecological networks

To demonstrate the practical relevance of our approach, we apply it to real-world networks obtained from Baldock et al., 2019 (presented in Section 2.1) and Baldock et al., 2011.

In a preliminary study (results not shown here), we first fitted the various colBiSBM models on the collection constituted of the four British networks introduced in Section 2.1. We obtained the following results: on this collection the iid-colBiSBM was selected as the best model, confirming the fact that they share a common organization. In that particular case, the assumption



of equal block proportions is adapted to the data. To strengthen our evaluation, we augmented the collection with a savanna pollination network deduced from the data collected in Kenya and presented in [Baldock et al., 2011](#). Although the original dataset focused on the daily temporal structure, we concatenated the data in a single merged network.

## 5.1 Joint estimation and partitioning of the five Baldock networks

We applied our partitioning method on those five networks, using the four models. The BIC-L obtained for the best partition and the various joint modeling are presented in Table 3.

Table 3 – BICL values for different models on the [Baldock et al., 2011, 2019](#) datasets.

Model	BICL ( $\uparrow$ )
iid-colBiSBM (Kenya and 4 British)	<b>−9466.866</b>
iid-colBiSBM on all networks	−9479.636
$\pi\rho$ -colBiSBM on all networks	−9497.920
Separate biSBM	−9620.375

Table 3 indicates that all our models beat the separate biSBM (last line) hence there is an advantage to model jointly those networks. The fact that the iid-colBiSBM on all networks is preferred to the  $\pi\rho$ -colBiSBM can be explained by the cost of all the additional free parameters for the  $\pi\rho$  that hinder its BIC-L. Finally, the preferred configuration is to split the networks in two partitions, one for the Kenyan network and another for the British networks. We can now interpret the results of the partitions obtained by the iid-colBiSBM and  $\pi\rho$ -colBiSBM models.

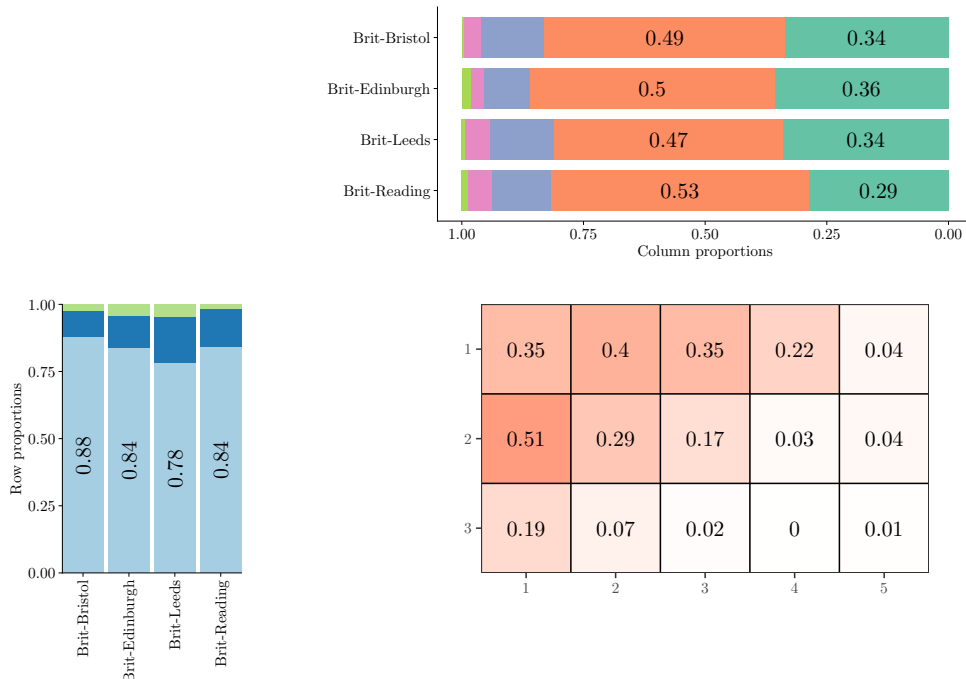


Figure 2 – Result of an iid-colBiSBM clustering applied to the five Baldock networks, four British and one Kenyan. Left is Kenyan network structure, right is shared British structure.

First, under the iid-colBiSBM, the clustering criterion (see Section 4.5) prefers to separate the Kenyan network from the British ones. Once partitioned, the method recovers a structure

commonly found in ecological networks: nestedness in both collections. In the Kenyan network, it identifies two groups of pollinators (row nodes) and two groups of plants (column nodes). The resulting connectivity matrix displays a reverse-stair pattern, with generalist species in both rows and columns interacting strongly among themselves (darker red shades,  $\alpha_{1,1} = 0.5$ ), while specialist species interact primarily with generalists ( $\alpha_{2,1}$  and  $\alpha_{1,2}$ ) and show minimal interaction with one another ( $\alpha_{2,2} = 0.02$ ). In terms of block sizes, the generalist species—although responsible for most of the interactions—form very small fractions of the network: only about 2% of the pollinators and 5% of the plants.

The structure for the British Baldock networks, shown in Figure 2, also exhibits nestedness with three groups of pollinators and five groups of plants. Interestingly the generalists connectivity coefficient is not the highest one, the highest one being with the second pollinator group. The generalist pollinators are distributed across blocks 1 and 2. Generalist plants are spread in 3 groups, 1, 2 and 3. When comparing to Figure 1, the joint modeling allows to refine the plant groups. In particular, it splits both generalists and specialists adding two new functional groups. Further analysis with ecologists may reveal the functional meaning of these new groups.

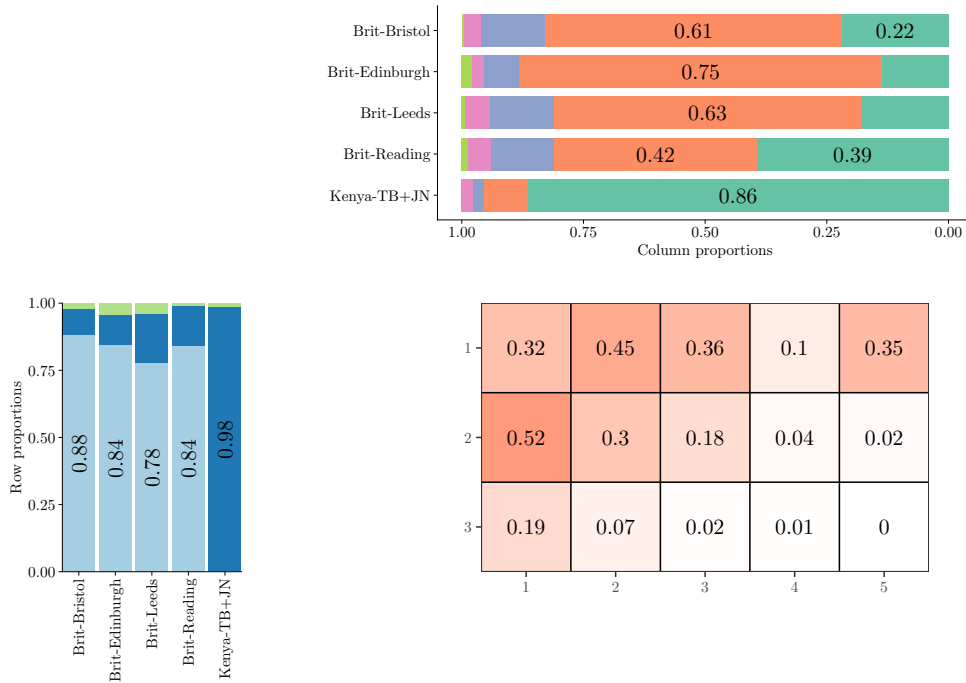


Figure 3 – Result of a  $\pi\rho$ -colBiSBM clustering applied to the five Baldock networks, four British and one Kenyan. The shared structure for the five networks is in shades of red. The networks are in this order: Bristol, Edinburgh, Leeds, Reading and Kenyan

Secondly, we perform the network collection partition using the  $\pi\rho$ -colBiSBM and plot the results in Figure 3. The flexibility induced by the varying block proportions leads to keeping together the five networks (whereas they were separated using the iid-colBiSBM) thus finding a shared structure between the Kenyan and British networks. Using this approach, the pollinator blocks are left unchanged but the plant blocks see at least a swap between blocks 4 and 5 along with some species of *former* block 4 joining *former* block 5. The Kenyan network does not populate the pollinator block 3 and sees most of its pollinators in block 2. For the plant blocks, it does not populate the first generalist block and the trend is reversed when comparing to British networks: the British networks populate block 4 and less block 5 whereas Kenyan network mainly (86%) make use of block 5 and not ( $< 10\%$ ) block 4. Note that, to go further,

interesting results could arise from comparing the nodes transfer between the two structures seen in Figures 2 and 3, since it could inform us on functional role change of the blocks between the clusterings. This ecological analysis is out of the scope of the present work.

## 5.2 Edge prediction on ecological networks

We now present a numerical experiment that demonstrates the benefits of joint modeling for predicting edges. We compare the results of our model-based approach to the performances obtained by a *Variational Graph AutoEncoder* (VGAE, Kipf and Welling, 2016). The objective is to prove that joint modeling leverages information transfer.

To do so, we consider the four British networks from Baldock et al., 2019 and randomly mask a proportion of edges on one of the four networks, then we gauge the predicted interactions. We use two kind of missing edges: missing links – i.e, we replace a random number of entries in the bi-adjacency matrix by a zero thus degrading the information by potentially masking ones– and missing dyads where we replace the value by a NA allowing the model to take into account that the “value of” the interactions are not known.

We fit the four colBiSBM models on the degraded networks. We also fit a biSBM on the degraded network: this plays the role of reference method where the information of the other networks cannot be leveraged. In order to challenge our probabilistic model based approach, we additionally fit a VGAE on the four British networks jointly or on the altered network. In a few words, we use a VGAE that takes as input features a non informative ordering of nodes as integers. The encoder has three GraphSAGE layers (Hamilton et al., 2018) of dimension 4 and the latent space is of dimension 4. The output of the encoder is two vectors  $V_1^m$  (for pollinators) and  $V_2^m$  (for plants) for each network.  $V_1^m$  (respectively  $V_2^m$ ) dimensions are  $(n_1^m, 4)$  (respectively  $(n_2^m, 4)$ ). For the decoder we use an inner product decoder as proposed by Kipf and Welling, 2016 adapted for bipartite networks. The predictions of the missing dyads or edges are done according to the fitting models. For missing dyads, we predict the unobserved (NA) dyads. For missing edges, we predict the altered edges.

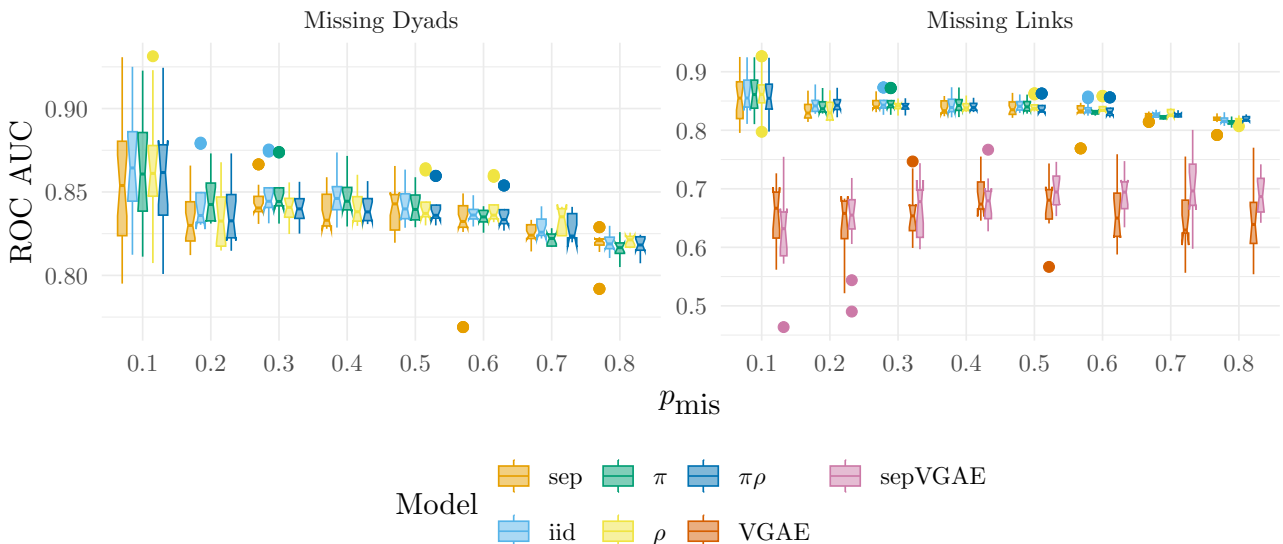


Figure 4 – *Information transfer on ecological data*: AUC of the recovered links in the missing dyads (left) and missing links (right). All the models are fitted on the Baldock British dataset with one of the networks altered. The “sep” model is a biSBM destined to serve as a reference.

In Figure 4 we plot the boxplots of the ROC AUC metrics. Our joint models perform

marginally better than the sep-biSBM for the recovery of the interactions thus indicating that the joint approach allow for information transfer between the networks. The best models are iid-colBiSBM and  $\pi$ -colBiSBM returning the higher AUC overall for the low  $p_{\text{mis}}$ .

From the two kinds of missing information, the missing dyad is the one that our models tackle best. We explain this by the fact that missing interactions are clearly labelled as NA and not taken into account to estimate the parameters. The block parameter estimation are then only based on observed interactions and nodes for which some interactions are missing in one network can be estimated by using the information for the block in the other networks. Whereas for the missing links experiment, the missing interactions are set as 0, potentially masking some interactions and being used to infer parameters, degrading the performance of the model for interaction prediction.

Regarding the VGAE, we observe that VGAE trained jointly on the 4 networks does not manage to transfer information. In both cases (sepVGAE and VGAE), the performances are far worse than the ones of the probabilistic model approach.

The difference between the sep-biSBM and colBiSBM models are narrow but we observe in the extensive simulation study that a nested structure (as the one observed in these ecological networks) is usually well retrieved by a sep-biSBM despite the alterations. However, for other network structures, we show that the differences can be clearer (see Section D.3).

## 6 Discussion

We introduce probabilistic models, namely colBiSBMs, that assume a shared connectivity structure among a collection of networks. The models range from the most constrained iid-colBiSBM to the more flexible  $\pi\rho$ -colBiSBM which accommodates empty blocks and varying block proportions. This joint modeling approach offers two main advantages compared to fitting separate biSBMs. First, by leveraging a larger combined dataset, the joint inference increases statistical power and can reveal finer structural patterns. Second, it establishes explicit links between the blocks (node clusters) identified in each network, allowing the corresponding clusters across networks to be interpreted as functional groups that play analogous roles within their respective ecosystems. This was illustrated in a dataset of five plant-pollinator networks.

Note that a limitation of the iid-colSBM is that all the networks of the collection must have the same global density. The other models are a bit more flexible in this regard. At present, unlike [Chabert-Liddell et al., 2024](#), our models do not incorporate a way to deal with common structures up to a density variation. Since there are many options to account for varying densities, we consider as a promising direction for future work to generalize the model by allowing any increasing function to mediate the transformation between network connectivity structures. This would enable a colBiSBM variant capable of identifying structural differences while explicitly accounting for density effects. Concretely, such a formulation would associate with each network an increasing function  $d_m$  that transforms the shared connectivity matrix  $\alpha$ , yielding the relation  $\alpha^m = d_m(\alpha)$ .

For the partition of a collection of networks, the example we develop in Section 5.1 can be attained by an exhaustive search (for 5 different elements there are 52 partitions). For larger collections, Bell numbers grow too rapidly to consider exhaustively searching for the best partition. We have then to resort to a partitioning algorithm like the one described in Section 4.5. In our simulation study (see Section D.4), we assess its capacity to retrieve the true partition of the collection of networks. However, the method reached its limits on the large collection of [Doré et al., 2021](#), presenting unstable behaviors. This may be due to the fact that there are numerous connectivity structures within this dataset and some of them are not as contrasted as in the simulation study. Some perspectives proposed by [Rebafka, 2023](#) could be adapted to bipartite networks.

# Acknowledgements

The authors are grateful to the INRAE MIGALE bioinformatics facility (MIGALE, INRAE, 2020. Migale bioinformatics Facility, doi: 10.15454/1.5572390655343293E12) for providing computing and storage resources. Louis Lacoste was funded by the MathNum department of INRAE and Fondation Mathématique Jacques Hadamard.

# References

- Agterberg, J., Lubberts, Z., & Arroyo, J. (2025). Joint Spectral Clustering in Multilayer Degree-Corrected Stochastic Blockmodels. *Journal of the American Statistical Association*, 1–15. <https://doi.org/10.1080/01621459.2025.2516201>
- Arroyo, J., Athreya, A., Cape, J., Chen, G., Priebe, C. E., & Vogelstein, J. T. (2021). Inference for Multiple Heterogeneous Networks with a Common Invariant Subspace. *Journal of Machine Learning Research*, 22(142), 1–49. Retrieved September 19, 2025, from <http://jmlr.org/papers/v22/19-558.html>
- Baldock, K. C. R., Goddard, M. A., Hicks, D. M., Kunin, W. E., Mitschunas, N., Morse, H., Osgathorpe, L. M., Potts, S. G., Robertson, K. M., Scott, A. V., Staniczenko, P. P. A., Stone, G. N., Vaughan, I. P., & Memmott, J. (2019). A systems approach reveals urban pollinator hotspots and conservation opportunities. *Nat Ecol Evol*, 3(3), 363–373. <https://doi.org/10.1038/s41559-018-0769-y>
- Baldock, K. C. R., Memmott, J., Ruiz-Guajardo, J. C., Roze, D., & Stone, G. N. (2011). Daily temporal structure in African savanna flower visitation networks and consequences for network sampling. *Ecology*, 92(3), 687–698. <https://doi.org/10.1890/10.1110.1>
- Biernacki, C., Celeux, G., & Govaert, G. (2000). Assessing a mixture model for clustering with the integrated completed likelihood. *IEEE Transactions on Pattern Analysis and Machine Intelligence*, 22(7), 719–725. <https://doi.org/10.1109/34.865189>
- Celisse, A., Daudin, J.-J., & Pierre, L. (2012). Consistency of maximum-likelihood and variational estimators in the stochastic block model. *Electronic Journal of Statistics*, 6, 1847–1899. <https://doi.org/10.1214/12-EJS729>
- Chabert-Liddell, S.-C., Barbillon, P., & Donnet, S. (2024). Learning common structures in a collection of networks. An application to food webs. *The Annals of Applied Statistics*, 18(2), 1213–1235. <https://doi.org/10.1214/23-AOAS1831>
- Chiquet, J., Donnet, S., & Barbillon, P. (2024, September 16). *Sbm: Stochastic Blockmodels* (Version 0.4.7). Retrieved November 4, 2024, from <https://cran.r-project.org/web/packages/sbm/index.html>
- Clauset, A., Moore, C., & Newman, M. E. J. (2008). Hierarchical structure and the prediction of missing links in networks. *Nature*, 453(7191), 98–101. <https://doi.org/10.1038/nature06830>
- Corso, G., De Araujo, A. I. L., & De Almeida, A. M. (2011). Connectivity and Nestedness in Bipartite Networks from Community Ecology. *J. Phys.: Conf. Ser.*, 285, 012009. <https://doi.org/10.1088/1742-6596/285/1/012009>
- Daudin, J.-J., Picard, F., & Robin, S. (2008). A mixture model for random graphs. *Stat Comput*, 18(2), 173–183. <https://doi.org/10.1007/s11222-007-9046-7>
- Doré, M., Fontaine, C., & Thébault, E. (2021). Relative effects of anthropogenic pressures, climate, and sampling design on the structure of pollination networks at the global scale. *Global Change Biology*, 27(6), 1266–1280. <https://doi.org/10.1111/gcb.15474>
- Elle, E., Elwell, S. L., & Gielens, G. A. (2012). The use of pollination networks in conservation<sup>1</sup>
- This article is part of a Special Issue entitled “Pollination biology research in Canada:

- Perspectives on a mutualism at different scales". *Botany*, 90(7), 525–534. <https://doi.org/10.1139/b11-111>
- Govaert, G., & Nadif, M. (2003). Clustering with block mixture models. *Pattern Recognition*, 36(2), 463–473. [https://doi.org/10.1016/S0031-3203\(02\)00074-2](https://doi.org/10.1016/S0031-3203(02)00074-2)
- Govaert, G., & Nadif, M. (2008). Block clustering with Bernoulli mixture models: Comparison of different approaches. *Computational Statistics & Data Analysis*, 52(6), 3233–3245. <https://doi.org/10.1016/j.csda.2007.09.007>
- Govaert, G., & Nadif, M. (2010). Latent Block Model for Contingency Table. *Communications in Statistics - Theory and Methods*, 39(3), 416–425. <https://doi.org/10.1080/03610920903140197>
- Hamilton, W. L., Ying, R., & Leskovec, J. (2018, September 10). *Inductive Representation Learning on Large Graphs*. arXiv: 1706.02216 [cs]. <https://doi.org/10.48550/arXiv.1706.02216>
- Hubert, L., & Arabie, P. (1985). Comparing partitions. *Journal of Classification*, 2(1), 193–218. <https://doi.org/10.1007/BF01908075>
- Kaszewska-Gilas, K., Kosicki, J. Z., Hromada, M., & Skoracki, M. (2021). Global Studies of the Host-Parasite Relationships between Ectoparasitic Mites of the Family Syringophilidae and Birds of the Order Columbiformes. *Animals*, 11(12), 3392. <https://doi.org/10.3390/ani11123392>
- Keribin, C., Brault, V., Celeux, G., & Govaert, G. (2015). Estimation and selection for the latent block model on categorical data. *Stat Comput*, 25(6), 1201–1216. <https://doi.org/10.1007/s11222-014-9472-2>
- Kipf, T. N., & Welling, M. (2016, November 21). *Variational Graph Auto-Encoders*. arXiv: 1611.07308 [stat]. <https://doi.org/10.48550/arXiv.1611.07308>
- Kumpulainen, I., Dalleiger, S., Vreeken, J., & Tatti, N. (2024, December 20). *From your Block to our Block: How to Find Shared Structure between Stochastic Block Models over Multiple Graphs*. arXiv: 2412.15476 [cs]. <https://doi.org/10.48550/arXiv.2412.15476>
- Leger, J.-B., Barbillon, P., & Chiquet, J. (2021, December 1). *Blockmodels: Latent and Stochastic Block Model Estimation by a 'V-EM' Algorithm* (Version 1.1.5). Retrieved November 4, 2024, from <https://cran.r-project.org/web/packages/blockmodels/index.html>
- Matias, C., & Miele, V. (2017). Statistical Clustering of Temporal Networks Through a Dynamic Stochastic Block Model. *J. R. Stat. Soc. Ser. B. Stat. Methodol.*, 79(4), 1119–1141. <https://doi.org/10.1111/rssb.12200>
- Michalska-Smith, M. J., & Allesina, S. (2019). Telling ecological networks apart by their structure: A computational challenge (T. Bollenbach, Ed.). *PLoS Comput Biol*, 15(6), e1007076. <https://doi.org/10.1371/journal.pcbi.1007076>
- Pavlopoulos, G. A., Kontou, P. I., Pavlopoulou, A., Bouyioukos, C., Markou, E., & Bagos, P. G. (2018). Bipartite graphs in systems biology and medicine: A survey of methods and applications. *GigaScience*, 7(4), giy014. <https://doi.org/10.1093/gigascience/giy014>
- Pichon, B., Le Goff, R., Morlon, H., & Perez-Lamarque, B. (2024). Telling mutualistic and antagonistic ecological networks apart by learning their multiscale structure. *Methods in Ecology and Evolution*, 15(6), 1113–1128. <https://doi.org/10.1111/2041-210X.14328>
- Rebafka, T. (2023). Model-based clustering of multiple networks with a hierarchical algorithm. *Stat Comput*, 34(1), 32. <https://doi.org/10.1007/s11222-023-10329-w>
- Sander, E. L., Wootton, J. T., & Allesina, S. (2015). What Can Interaction Webs Tell Us About Species Roles? *PLoS Computational Biology*, 11(7), e1004330. <https://doi.org/10.1371/journal.pcbi.1004330>
- Sheykhal, S., Fernández-Gracia, J., Traveset, A., Ziegler, M., Voolstra, C. R., Duarte, C. M., & Eguíluz, V. M. (2020). Robustness to extinction and plasticity derived from mutualistic bipartite ecological networks. *Sci Rep*, 10(1), 9783. <https://doi.org/10.1038/s41598-020-66131-5>



- Web of Life: Ecological networks database*. (2022, July). Retrieved June 17, 2023, from <https://www.web-of-life.es/map.php>
- Wills, P., & Meyer, F. G. (2020). Metrics for graph comparison: A practitioner’s guide. *PLOS ONE*, 15(2), e0228728. <https://doi.org/10.1371/journal.pone.0228728>
- Xu, M. (2021). Understanding Graph Embedding Methods and Their Applications. *SIAM Rev.*, 63(4), 825–853. <https://doi.org/10.1137/20M1386062>
- Zhou, T., Lü, L., & Zhang, Y.-C. (2009). Predicting missing links via local information. *Eur. Phys. J. B*, 71(4), 623–630. <https://doi.org/10.1140/epjb/e2009-00335-8>

## A Proof of the identifiability result

Along with results presented in Property 1 we also have the identifiability results for  $\pi$ -colBiSBM and  $\rho$ -colBiSBM shown in Property 2.

**Property 2.**  $\pi$ -colBiSBM *The parameters  $\theta = (\pi^1, \dots, \pi^M, \rho, \alpha)$  are identifiable up to a label switching of the blocks if those conditions are achieved:*

$$(2.1) \quad \forall m \in \{1, \dots, M\} : n_1^m \geq 2Q_2 - 1 \text{ and } \exists m^* \in \{1, \dots, M\} : n_2^{m^*} \geq 2Q_1 - 1.$$

$$(2.2) \quad \text{The coordinates of the vector } \alpha\rho \text{ are distinct.}$$

$$(2.3) \quad \forall m \in \{1, \dots, M\}, \text{ the coordinates of vector } (\bar{\pi}^m)^\top \bar{\alpha}^m \text{ are distinct.}$$

$$(2.4) \quad \text{The coordinates of the vector } \rho \text{ are distinct.}$$

$\rho$ -colBiSBM *The parameters  $\theta = (\pi, \rho^1, \dots, \rho^M, \alpha)$  are identifiable up to a label switching of the blocks if those conditions are achieved:*

$$(3.1) \quad \exists m^* \in \{1, \dots, M\} : n_1^{m^*} \geq 2Q_2 - 1 \text{ and } \forall m \in \{1, \dots, M\} : n_2^m \geq 2Q_1 - 1.$$

$$(3.2) \quad \forall m \in \{1, \dots, M\}, \text{ the coordinates of vector } \bar{\alpha}^m \bar{\rho}^m \text{ are distinct.}$$

$$(3.3) \quad \text{The coordinates of the vector } \pi^\top \alpha \text{ are distinct.}$$

$$(3.4) \quad \text{The coordinates of the vector } \pi \text{ are distinct.}$$

*Proof.* We derive the results in Properties 1 and 2.

iid-colBiSBM [Keribin et al., 2015](#) building on [Celisse et al., 2012](#), proved that the parameters  $(\pi^m, \rho^m, \alpha^m)$  of the  $\mathcal{F}$ -biSBM $_{n_1^m, n_2^m}(Q_1^m, Q_2^m, \pi^m, \rho^m, \alpha^m)$  are identifiable from the observation of network  $X^m$  when  $\mathcal{F}$  is the Bernoulli distribution and the following conditions are met:

1.  $n_1^m \geq 2Q_2^m - 1$  and  $n_2^m \geq 2Q_1^m - 1$ .
2.  $\forall 1 \leq q \leq Q_1^m, \pi_q^m > 0$  and the coordinates of vector  $\alpha^m \rho^m$  are distinct.
3.  $\forall 1 \leq r \leq Q_2^m, \rho_r^m > 0$  and the coordinates of vector  $(\pi^m)^\top \alpha^m$  are distinct.

Under the iid-colBiSBM model, for all  $m = 1 \dots M$ ,  $X^m \sim \mathcal{F}$ -biSBM $_{n_1^m, n_2^m}(Q_1, Q_2, \pi, \rho, \alpha)$ . This means that applying [Keribin et al., 2015](#), the identifiability of  $\alpha$ ,  $\pi$  and  $\rho$  is obtained from the distribution of  $X^{m^*}$  under assumptions (1.1) to (1.3).

$\pi$ -colBiSBM Under  $\pi$ -colBiSBM, we have for all  $m$ ,

$$X^m \sim \mathcal{F}\text{-biSBM}_{n_1^m, n_2^m}(Q_1^m, Q_2, \bar{\pi}^m, \rho, \bar{\alpha}^m)$$

where  $\bar{\pi}^m$  is the vector of non-zero proportions of length  $Q_1^m$  in  $\pi$  and  $\bar{\alpha}^m$  is the restriction of  $\alpha$  to the set  $\mathcal{Q}_1^m$ , i.e., the rows  $(\alpha_{qr})_{1 \leq r \leq Q_2}$  with  $q \in \mathcal{Q}_1^m$ . Under assumptions (2.1) to (2.3) and by noticing that (2.2) implies that  $\forall m \in \{1, \dots, M\}$ , the coordinates of vector  $\bar{\alpha}^m \rho$  are distinct, applying [Keribin et al., 2015](#) allows us to identify  $\bar{\alpha}^m$ ,  $\bar{\pi}^m$  and  $\rho$  for each of the networks  $X^m$ . From the  $\bar{\alpha}^m$  we build  $\alpha$  the complete matrix that merges the  $\bar{\alpha}^m$ . This is done by starting from any of the  $\bar{\alpha}^m$  and adding the missing entries from the others  $\bar{\alpha}^{m'}$  using assumption (2.4) to reorder the columns and assumption (2.2) to reorder the rows. This way we build  $\alpha$  and have the index matches to define  $\phi_m : \{1, \dots, Q_1^m\} \rightarrow \{1, \dots, Q_1\}$  such that  $\bar{\alpha}_{\phi_m(q), r}^m = \alpha_{qr}$ . Finally, we define  $\pi^m$  as follows:

$$\pi_q^m = \begin{cases} 0 & \forall q \in \{1, \dots, Q_1\} \setminus \phi_m(\{1, \dots, Q_1^m\}) \\ \bar{\pi}_{\phi_m^{-1}(q)}^m & \forall q \in \phi_m(\{1, \dots, Q_1^m\}) \end{cases}.$$

$\rho$ -colBiSBM Under  $\rho$ -colBiSBM, we have for all  $m$ ,

$$X^m \sim \mathcal{F}\text{-biSBM}_{n_1^m, n_2^m}(Q_1, Q_2^m, \boldsymbol{\pi}, \bar{\boldsymbol{\rho}}^m, \bar{\boldsymbol{\alpha}}^m)$$

where  $\bar{\boldsymbol{\rho}}^m$  is the vector of non-zero proportions of length  $Q_2^m$  in  $\boldsymbol{\rho}$  and  $\bar{\boldsymbol{\alpha}}^m$  is the restriction of  $\boldsymbol{\alpha}$  to the set  $Q_2^m$ , i.e., the columns  $(\alpha_{qr})_{1 \leq q \leq Q_1}$  with  $r \in Q_2^m$ . By applying [Keribin et al., 2015](#) using assumptions (3.1) to (3.3) and noticing that (3.3) implies that  $\forall m \in \{1, \dots, M\}$ , the coordinates of vector  $\boldsymbol{\pi}^\top \bar{\boldsymbol{\alpha}}^m$  are distinct, we identify  $\bar{\boldsymbol{\alpha}}^m$ ,  $\bar{\boldsymbol{\rho}}^m$  and  $\boldsymbol{\pi}$  for each of the networks  $X^m$ . From the  $\bar{\boldsymbol{\alpha}}^m$  we build  $\boldsymbol{\alpha}$  the complete matrix that merges the  $\bar{\boldsymbol{\alpha}}^m$ . This is done by starting from any of the  $\bar{\boldsymbol{\alpha}}^m$  and adding the missing entries from the others  $\bar{\boldsymbol{\alpha}}^{m'}$  using assumption (3.4) to reorder the rows and assumption (3.3) to reorder the columns. This way we build  $\boldsymbol{\alpha}$  and have the index matches to define  $\psi_m : \{1, \dots, Q_2^m\} \rightarrow \{1, \dots, Q_2\}$  such that  $\bar{\alpha}_{q\psi_m(r)}^m = \alpha_{qr}$ . Finally, we define  $\boldsymbol{\rho}^m$  as follows:

$$\rho_r^m = \begin{cases} 0 & \forall r \in \{1, \dots, Q_2\} \setminus \psi_m(\{1, \dots, Q_2^m\}) \\ \bar{\rho}_{\psi_m^{-1}(r)}^m & \forall r \in \psi_m(\{1, \dots, Q_2^m\}) \end{cases}.$$

$\pi\rho$ -colBiSBM Under  $\pi\rho$ -colBiSBM, we have for all  $m$ ,

$$X^m \sim \mathcal{F}\text{-biSBM}_{n_1^m, n_2^m}(Q_1^m, Q_2^m, \bar{\boldsymbol{\pi}}^m, \bar{\boldsymbol{\rho}}^m, \bar{\boldsymbol{\alpha}}^m)$$

where  $\bar{\boldsymbol{\pi}}^m$  is the vector of non-zero proportions of length  $Q_1^m$  in  $\boldsymbol{\pi}$ ,  $\bar{\boldsymbol{\rho}}^m$  is the vector of non-zero proportions of length  $Q_2^m$  in  $\boldsymbol{\rho}$  and  $\bar{\boldsymbol{\alpha}}^m$  is the restriction of  $\boldsymbol{\alpha}$  to the set  $Q_1^m \times Q_2^m$ , i.e.,  $(\alpha_{qr})_{q \in Q_1^m, r \in Q_2^m}$ . By applying [Keribin et al., 2015](#) using assumptions (2.1) to (2.3) we have the identifiability of each of the  $X^m$  networks. The difficulty lies in the reordering of the blocks across the networks and the fact that the  $\bar{\boldsymbol{\alpha}}^m$  only represent subparts of the  $\boldsymbol{\alpha}$  matrix. Under assumption (2.4) one can build  $\boldsymbol{\alpha}$  from the  $\bar{\boldsymbol{\alpha}}^m$ .

Start by taking  $\bar{\boldsymbol{\alpha}}^1$  as the first  $\boldsymbol{\alpha}$ . Then for each  $m \in \{2, \dots, M\}$ , find common entries with the current  $\boldsymbol{\alpha}$ , from it deduce the permutations of rows and columns for  $\bar{\boldsymbol{\alpha}}^m$  that will allow to match the entries. If there are new entries add them to the current  $\boldsymbol{\alpha}$  either from the permutations, either at the end of the rows and/or columns. Update the previous index matches from previous networks that where possibly changed and repeat for next  $m$ . As mentioned in Section 3.2 some row and column groups may never interact and thus  $\boldsymbol{\alpha}$  would be incomplete.

Building  $\boldsymbol{\alpha}$  in this manner gives us the index matches and thus define  $\phi_m : \{1, \dots, Q_1^m\} \rightarrow \{1, \dots, Q_1\}$  and  $\psi_m : \{1, \dots, Q_2^m\} \rightarrow \{1, \dots, Q_2\}$  such that  $\bar{\alpha}_{\phi_m(q)\psi_m(r)}^m = \alpha_{qr}$ . Finally, we define  $\boldsymbol{\pi}^m$  and  $\boldsymbol{\rho}^m$  as follows:

$$\begin{aligned} \pi_q^m &= \begin{cases} 0 & \forall q \in \{1, \dots, Q_1\} \setminus \phi_m(\{1, \dots, Q_1^m\}) \\ \bar{\pi}_{\phi_m^{-1}(q)}^m & \forall q \in \phi_m(\{1, \dots, Q_1^m\}) \end{cases} \quad \text{and} \\ \rho_r^m &= \begin{cases} 0 & \forall r \in \{1, \dots, Q_2\} \setminus \psi_m(\{1, \dots, Q_2^m\}) \\ \bar{\rho}_{\psi_m^{-1}(r)}^m & \forall r \in \psi_m(\{1, \dots, Q_2^m\}) \end{cases}. \end{aligned}$$

□

## B On the model selection criterion

For  $\pi\rho$ -colBiSBM, the model is described by its supports  $S^{(1)}, S^{(2)}$ . Let us denote both supports by  $S^{(1,2)}$ .

$$\begin{aligned}
p(\mathbf{X}, \mathbf{Z}, \mathbf{W} \mid S^{(1,2)}) &= \int_{\boldsymbol{\theta}_{S^{(1,2)}}} p(\mathbf{X}, \mathbf{Z}, \mathbf{W} \mid S^{(1,2)}) p(\boldsymbol{\theta}_{S^{(1,2)}}) d\boldsymbol{\theta}_{S^{(1,2)}} \\
&= \int_{\boldsymbol{\alpha}_{S^{(1,2)}}} \int_{\boldsymbol{\pi}_{S^{(1)}}} \int_{\boldsymbol{\rho}_{S^{(2)}}} p(\mathbf{X} \mid \mathbf{Z}, \mathbf{W}, S^{(1,2)}) p(\mathbf{Z} \mid \boldsymbol{\pi}_{S^{(1)}}, S^{(1)}) p(\mathbf{W} \mid \boldsymbol{\rho}_{S^{(2)}}, S^{(2)}) \\
&\quad p(\boldsymbol{\alpha}_{S^{(1,2)}}) p(\boldsymbol{\pi}_{S^{(1)}}) p(\boldsymbol{\rho}_{S^{(2)}}) d\boldsymbol{\alpha}_{S^{(1,2)}} d\boldsymbol{\pi}_{S^{(1)}} d\boldsymbol{\rho}_{S^{(2)}} \\
&= \underbrace{\int_{\boldsymbol{\alpha}_{S^{(1,2)}}} p(\mathbf{X} \mid \mathbf{Z}, \mathbf{W}, \boldsymbol{\alpha}_{S^{(1,2)}}, S^{(1,2)}) p(\boldsymbol{\alpha}_{S^{(1,2)}}) d\boldsymbol{\alpha}_{S^{(1,2)}}}_A \\
&\quad \times \underbrace{\int_{\boldsymbol{\pi}_{S^{(1)}}} p(\mathbf{Z} \mid \boldsymbol{\pi}_{S^{(1)}}, S^{(1)}) d\boldsymbol{\pi}_{S^{(1)}}}_{B1} \times \underbrace{\int_{\boldsymbol{\rho}_{S^{(2)}}} p(\mathbf{W} \mid \boldsymbol{\rho}_{S^{(2)}}, S^{(2)}) d\boldsymbol{\rho}_{S^{(2)}}}_{B2}, \tag{S-1}
\end{aligned}$$

We use a BIC approximation on  $A$ :

$$\begin{aligned}
A = p(\mathbf{X} \mid \mathbf{Z}, \mathbf{W}, S^{(1,2)}) &= \int_{\boldsymbol{\alpha}_{S^{(1,2)}}} \left( \prod_{m=1}^M p(X^m \mid Z^m, W^m; \boldsymbol{\alpha}_{S^{(1,2)}}, S^{(1,2)}) \right) p(\boldsymbol{\alpha}_{S^{(1,2)}}) d\boldsymbol{\alpha}_{S^{(1,2)}} \\
&\approx \max_{\boldsymbol{\alpha}_{S^{(1,2)}}} \exp \left( \sum_{m=1}^M \ell(X^m \mid Z^m, W^m; \boldsymbol{\alpha}_{S^{(1,2)}}, S^{(1,2)}) \right. \\
&\quad \left. - \underbrace{\frac{1}{2} \sum_{q \in Q_1} \sum_{r \in Q_2} \mathbb{1}_{((S^{(1)})', S^{(2)})_{qr} > 0}}_{\dim(\boldsymbol{\alpha}_{S^{(1,2)}})} \log \left( \sum_{m=1}^M n_1^m n_2^m \right) + \mathcal{O}(1) \right).
\end{aligned}$$

For  $B1$  and  $B2$  we propose a  $Q_i^m$ -dimensional Dirichlet prior for each mixture parameter:

$$\begin{aligned}
B1 = p(\mathbf{Z} \mid S^{(1)}) &= \prod_{m=1}^M \int_{\boldsymbol{\pi}_{S^{(1)}}^m} p(Z^m \mid \boldsymbol{\pi}_{S^{(1)}}^m) p(\boldsymbol{\pi}_{S^{(1)}}^m) d\boldsymbol{\pi}_{S^{(1)}}^m \\
&\approx \max_{\boldsymbol{\pi}_{S^{(1)}}} \exp \left( \sum_{m=1}^M \ell(Z^m; \boldsymbol{\pi}_{S^{(1)}}) - \frac{Q_1^m - 1}{2} \log(n_1^m) + \mathcal{O}(1) \right), \\
B2 = p(\mathbf{W} \mid S^{(2)}) &= \prod_{m=1}^M \int_{\boldsymbol{\rho}_{S^{(2)}}^m} p(W^m \mid \boldsymbol{\rho}_{S^{(2)}}^m) p(\boldsymbol{\rho}_{S^{(2)}}^m) d\boldsymbol{\rho}_{S^{(2)}}^m \\
&\approx \max_{\boldsymbol{\rho}_{S^{(2)}}} \exp \left( \sum_{m=1}^M \ell(W^m; \boldsymbol{\rho}_{S^{(2)}}) - \frac{Q_2^m - 1}{2} \log(n_2^m) + \mathcal{O}(1) \right).
\end{aligned}$$

Then, using the log of (S-1) and inputting  $A, B1$  and  $B2$ :

$$\begin{aligned}
\log p(\mathbf{X}, \mathbf{Z}, \mathbf{W} \mid S^{(1,2)}) &\approx \max_{\boldsymbol{\alpha}_{S^{(1,2)}}} \left( \sum_{m=1}^M \ell(X^m \mid Z^m, W^m; \boldsymbol{\alpha}_{S^{(1,2)}}, S^{(1,2)}) \right. \\
&\quad \left. - \frac{1}{2} \sum_{q,r=1}^{Q_1, Q_2} \mathbb{1}_{((S^{(1)})', S^{(2)})_{qr} > 0} \log \left( \sum_{m=1}^M n_1^m n_2^m \right) \right) \\
&\quad + \max_{\boldsymbol{\pi}_{S^{(1)}}} \left( \sum_{m=1}^M \ell(Z^m; \boldsymbol{\pi}_{S^{(1)}}) - \frac{Q_1^m - 1}{2} \log(n_1^m) \right) \\
&\quad + \max_{\boldsymbol{\rho}_{S^{(2)}}} \left( \sum_{m=1}^M \ell(W^m; \boldsymbol{\rho}_{S^{(2)}}) - \frac{Q_2^m - 1}{2} \log(n_2^m) \right) \\
&\approx \max_{\boldsymbol{\theta}_{S^{(1,2)}}} \sum_{m=1}^M \left[ \ell(X^m \mid Z^m, W^m, S^{(1,2)}; \boldsymbol{\alpha}_{S^{(1,2)}}) + \ell(Z^m; \boldsymbol{\pi}_{S^{(1)}}) + \ell(W^m; \boldsymbol{\rho}_{S^{(2)}}) \right] \\
&\quad - \frac{1}{2} \left( \sum_{m=1}^M (Q_1^m - 1) \log(n_1^m) + \sum_{m=1}^M (Q_2^m - 1) \log(n_2^m) \right. \\
&\quad \left. + \sum_{q=1}^{Q_1} \sum_{r=1}^{Q_2} \mathbb{1}_{((S^{(1)})', S^{(2)})_{qr} > 0} \log \left( \sum_{m=1}^M n_1^m n_2^m \right) \right) \\
&\approx \max_{\boldsymbol{\theta}_{S^{(1,2)}}} \ell(\mathbf{X}, \mathbf{Z}, \mathbf{W} \mid S^{(1,2)}; \boldsymbol{\theta}_{S^{(1,2)}}) \\
&\quad - \frac{1}{2} [\text{pen}_{\pi}(Q_1, S^{(1)}) + \text{pen}_{\rho}(Q_2, S^{(2)}) + \text{pen}_{\alpha}(Q_1, Q_2, S^{(1,2)})]. \tag{S-2}
\end{aligned}$$

Recalling that the penalties are:

$$\text{pen}_{\pi}(Q_1, S^{(1)}) = \sum_{m=1}^M (Q_1^m - 1) \log n_1^m, \quad \text{pen}_{\rho}(Q_2, S^{(2)}) = \sum_{m=1}^M (Q_2^m - 1) \log n_2^m,$$

and

$$\text{pen}_{\alpha}(Q_1, Q_2, S^{(1,2)}) = \left( \sum_{q=1}^{Q_1} \sum_{r=1}^{Q_2} \mathbb{1}_{((S^{(1)})', S^{(2)})_{qr} > 0} \right) \log(N_M),$$

with  $N_M = \sum_{m=1}^M n_1^m n_2^m$ . As  $\mathbf{Z}$  and  $\mathbf{W}$  are unknown we replace the  $Z_{iq}^m, W_{jr}^m$  by their corresponding variational parameters  $\tau_{iq}^{1,m}, \tau_{jr}^{2,m}$ :

$$\begin{aligned}
\log p(\mathbf{X}, \mathbf{Z}, \mathbf{W} \mid S^{(1,2)}) &\approx \max_{\boldsymbol{\theta}_{S^{(1,2)}}} \mathbb{E}_{\hat{\mathcal{R}}} [\ell(\mathbf{X}, \mathbf{Z}, \mathbf{W} \mid S^{(1,2)}; \boldsymbol{\theta}_{S^{(1,2)}})] \\
&\quad - \frac{1}{2} [\text{pen}_{\pi}(Q_1, S^{(1)}) + \text{pen}_{\rho}(Q_2, S^{(2)}) + \text{pen}_{\alpha}(Q_1, Q_2, S^{(1,2)})] \\
&=: \text{ICL}(\mathbf{X}, Q_1, Q_2, S^{(1,2)})
\end{aligned}$$

To obtain the criterion BIC-L( $\mathbf{X}, Q_1, Q_2$ ) we need to penalize for the supports  $S^{(1)}, S^{(2)}$ . For a given  $Q_i$  blocks, where  $i \in \{1, 2\}$ , we set the prior on  $S^{(i)}$  to be the product of uniform priors for the number of blocks  $Q_i^m$  populated by the network  $m$  and uniform priors for the actual choice of the  $Q_i^m$  blocks (i.e., the position of ones in the  $m$ th row of  $S^{(i)}$ ) among the  $Q_i$  possible blocks:

$$p_{Q_i}(S^{(i)}) = p_{Q_i}(Q_1, \dots, Q_M) \cdot p_{Q_i}(S^{(i)} \mid Q_1, \dots, Q_M) = \frac{1}{Q_i^M} \prod_{m=1}^M \frac{1}{\binom{Q_i}{Q_i^m}}$$

Using a BIC approximation and under a concentration assumption on the correct supports we obtain:

$$\begin{aligned}\log p(\mathbf{X}, \mathbf{Z}, \mathbf{W}) &= \log \int_{S^{(1)}} \int_{S^{(2)}} p(\mathbf{X}, \mathbf{Z}, \mathbf{W} \mid S^{(1,2)}) p_{Q_1}(S^{(1)}) p_{Q_2}(S^{(2)}) dS^{(1)} dS^{(2)} \\ &\approx \log \int_{S^{(1)}} \int_{S^{(2)}} \exp[\text{ICL}(\mathbf{X}, Q_1, Q_2, S^{(1,2)}) + \log(p_{Q_1}(S^{(1)})) + \log(p_{Q_2}(S^{(2)}))] dS^{(1)} dS^{(2)} \\ &\approx \max_{S^{(1)} \in \mathcal{S}_{Q_1}, S^{(2)} \in \mathcal{S}_{Q_2}} [\text{ICL}(\mathbf{X}, Q_1, Q_2, S^{(1,2)}) + \log(p_{Q_1}(S^{(1)})) + \log(p_{Q_2}(S^{(2)}))].\end{aligned}$$

Recalling that:

$$\begin{aligned}\ell(\mathbf{X}, \mathbf{Z}, \mathbf{W}; \boldsymbol{\theta}_{S^{(1,2)}}) &= \log p(\mathbf{Z}, \mathbf{W} \mid \mathbf{X}; \boldsymbol{\theta}_{S^{(1,2)}}) + \ell(\mathbf{X}; \boldsymbol{\theta}_{S^{(1,2)}}) \\ &\Rightarrow \mathbb{E}_{\mathbf{Z}, \mathbf{W} \mid \mathbf{X}}[\ell(\mathbf{X}, \mathbf{Z}, \mathbf{W}; \boldsymbol{\theta}_{S^{(1,2)}})] = -\mathcal{H}(p(\mathbf{Z}, \mathbf{W} \mid \mathbf{X}; \boldsymbol{\theta}_{S^{(1,2)}})) + \ell(\mathbf{X}; \boldsymbol{\theta}_{S^{(1,2)}}),\end{aligned}$$

and under the variational approximation, namely approximating  $\mathbf{Z}, \mathbf{W} \mid \mathbf{X}$  by  $\hat{\mathcal{R}}$ :

$$\mathbb{E}_{\hat{\mathcal{R}}}[\ell(\mathbf{X}, \mathbf{Z}, \mathbf{W}; \boldsymbol{\theta}_{S^{(1,2)}})] = \ell(\mathbf{X}; \boldsymbol{\theta}_{S^{(1,2)}}) - \mathcal{H}(\hat{\mathcal{R}}).$$

Thus the ICL can be expressed as:

$$\begin{aligned}\text{ICL}(\mathbf{X}, Q_1, Q_2, S^{(1,2)}) &= \max_{\boldsymbol{\theta}_{S^{(1,2)}}} \ell(\mathbf{X}; \boldsymbol{\theta}_{S^{(1,2)}}) - \mathcal{H}(\hat{\mathcal{R}}) \\ &\quad - \frac{1}{2} [\text{pen}_{\pi}(Q_1, S^{(1)}) + \text{pen}_{\rho}(Q_2, S^{(2)}) + \text{pen}_{\alpha}(Q_1, Q_2, S^{(1,2)})]\end{aligned}$$

Finally in order to obtain the BIC-L criterion, we add the entropy of the surrogate distribution as the ICL penalizes on the entropy and in order to allow fuzzy node memberships we want to alleviate this penalization. By denoting  $\text{pen}_{S^{(i)}}(Q_i) = -2 \log p_{Q_i}(S^{(i)})$  and recalling that  $\mathcal{J}(\hat{\mathcal{R}}, \boldsymbol{\theta}_{S^{(1,2)}}) = \mathbb{E}_{\hat{\mathcal{R}}}[\ell(\mathbf{X}, \mathbf{Z}, \mathbf{W}; \boldsymbol{\theta}_{S^{(1,2)}})] + \mathcal{H}(\hat{\mathcal{R}})$ , the criterion is:

$$\begin{aligned}\text{BIC-L}(\mathbf{X}, Q_1, Q_2) &= \max_{\substack{S^{(1)} \in \mathcal{S}_{Q_1} \\ S^{(2)} \in \mathcal{S}_{Q_2}}} \left[ \max_{\boldsymbol{\theta}_{S^{(1,2)}}} \mathcal{J}(\hat{\mathcal{R}}, \boldsymbol{\theta}_{S^{(1,2)}}) - \frac{1}{2} [\text{pen}_{\pi}(Q_1, S^{(1)}) + \text{pen}_{\rho}(Q_2, S^{(2)}) \right. \\ &\quad \left. + \text{pen}_{\alpha}(Q_1, Q_2, S^{(1,2)}) \right. \\ &\quad \left. + \text{pen}_{S^{(1)}}(Q_1) + \text{pen}_{S^{(2)}}(Q_2) \right].\end{aligned}$$

## C Details of the partitioning algorithm

Continuing Section 4.5, the principle is to adjust the colBiSBM model over the full collection of  $M$  networks and then compute the dissimilarity matrix between all networks of the collection. We obtain the collection  $\mathcal{G} = \{1, \dots, M\}$  the trivial partition in a unique group.

The parameters for the dissimilarity are defined as follows:

$$\begin{aligned}\tilde{n}_{qr}^m &= \sum_{i=1}^{n_1^m} \sum_{j=1}^{n_2^m} \hat{\tau}_{iq}^{1,m} \hat{\tau}_{jr}^{2,m}, & \tilde{\alpha}_{qr}^m &= \frac{\sum_{i=1}^{n_1^m} \sum_{j=1}^{n_2^m} \hat{\tau}_{iq}^{1,m} \hat{\tau}_{jr}^{2,m} X_{ij}^m}{\tilde{n}_{qr}^m}, \\ \tilde{\pi}_q^m &= \frac{\sum_{i=1}^{n_1^m} \hat{\tau}_{iq}^{1,m}}{n_1^m}, & \tilde{\rho}_r^m &= \frac{\sum_{j=1}^{n_2^m} \hat{\tau}_{jr}^{2,m}}{n_2^m}.\end{aligned}$$

And the pairwise dissimilarity for networks  $(m, m') \in \{1, \dots, M\}^2$  is then:

$$D_{\mathcal{M}}(m, m') = \sum_{q=1}^{Q_1} \sum_{r=1}^{Q_2} \max(\tilde{\pi}_q^m, \tilde{\pi}_q^{m'}) \left( \tilde{\alpha}_{qr}^m - \tilde{\alpha}_{qr}^{m'} \right)^2 \max(\tilde{\rho}_r^m, \tilde{\rho}_r^{m'}).$$



Then using a hierarchical clustering we split the collection in two sub-collections with the dissimilarity matrix. On the two subcollections we adjust a colBiSBM model and we compute the score of this new partition  $\mathcal{G}^* = \{G_1, G_2\}$ . If  $Sc(\mathcal{G}^*) > Sc(\mathcal{G})$ , we repeat the same procedure on  $G_1$  and  $G_2$ . Else we return  $\mathcal{G}$ . We illustrate our capacity to perform a partition of a simulated collection for all colBiSBM models, results are presented in figure S-8 and illustrate that as soon as the structure is sufficiently marked ( $\epsilon_\alpha \geq 0.3$ ) clustering is almost perfect. For all details on the experiment see Section D.4.

## D Details of the numerical experiments

In this section, we conduct a comprehensive simulation study to evaluate the accuracy of our inference procedure and to assess our ability to distinguish between the various competing models. Additionally, we demonstrate the benefits of jointly modeling multiple networks, particularly in terms of improved link prediction performance.

**Reproducibility** All the codes used to simulate and to perform the analysis can be found at <https://github.com/Polarolouis/code-colbisbm/>.

### D.1 Assessing the quality of estimation

We first assess our ability to fit the most complex model namely the  $\pi\rho$ -colBiSBM in our framework. To do so, we simulate networks with varying degrees of structural clarity and evaluate how well the model recovers the underlying node clusters. Clustering is a central feature in network analysis, and its quality is quantified using the Adjusted Rand Index (ARI). We begin by describing the simulation settings, then introduce the quality indicators, and finally present the results. Some tables are deferred to the Supplementary Material section for clarity.

**Simulation settings** We set  $M = 2$  and simulate bipartite networks involving  $n_1^m = 240$  nodes in row and  $n_2^m = 240$  nodes in column with  $Q_1 = 4$  blocks in row and  $Q_2 = 4$  blocks in columns. The connection matrix  $\alpha$  is set as follows:

$$\alpha = .25 + \begin{pmatrix} 3\epsilon_\alpha & 2\epsilon_\alpha & \epsilon_\alpha & -\epsilon_\alpha \\ 2\epsilon_\alpha & 2\epsilon_\alpha & -\epsilon_\alpha & \epsilon_\alpha \\ \epsilon_\alpha & -\epsilon_\alpha & \epsilon_\alpha & 2\epsilon_\alpha \\ -\epsilon_\alpha & \epsilon_\alpha & 2\epsilon_\alpha & 0 \end{pmatrix},$$

with  $\epsilon_\alpha$  taking nine equally spaced values ranging from 0 to 0.24.  $\epsilon_\alpha$  represents the strength of the network structure. If  $\epsilon_\alpha = 0$ , the model is an Erdős–Rényi model with a constant probability of connexion between any pair of nodes. As  $\epsilon_\alpha$  increases, the differences between the blocks become more pronounced, leading to a clearer underlying structure in the network.

For each unique combination of parameters, we perform  $N = 3$  repetitions under the model  $\text{Bern-BiSBM}_{240,240}(4, 4, \alpha, \pi^m, \rho^m)$  where the block proportions  $(\pi^m)_{m=1,2}$  and  $(\rho^m)_{m=1,2}$  are chosen as follows

$$\begin{aligned} \pi^1 &= \sigma_1 (0.2 \quad 0.4 \quad 0.4 \quad 0), & \pi^2 &= (0.25 \quad 0.25 \quad 0.25 \quad 0.25), \\ \rho^1 &= (0.25 \quad 0.25 \quad 0.25 \quad 0.25), & \rho^2 &= \sigma_2 (0 \quad 0.33 \quad 0.33 \quad 0.33), \end{aligned}$$

where  $\sigma_1$  and  $\sigma_2$  are two permutations of  $\{1, \dots, 4\}$  randomly chosen for each one of the 3 repetitions. This allows to randomly affect the non-present block in each simulation.

**Inference** For each network, we put in competition the five models iid-colBiSBM,  $\pi$ -colBiSBM,  $\rho$ -colBiSBM,  $\pi\rho$ -colBiSBM *sep-biSBM*. The parameters are estimated with the VEM algorithm described in Section 4.3. The numbers of blocks  $Q_1$  and  $Q_2$  and if necessary the supports  $S^1$  and  $S^2$  are selected with the BIC-L criterion. The BIC-L is also used to chose among the five models.

**Results** Figure S-1 proves that the  $\pi\rho$ -colBiSBM is the preferred model if the networks' block structure is clear enough. In case where  $\epsilon_\alpha$  is very small, all the blocks are equivalent and the best model is the iid-colBiSBM.

Table S-1 provides the frequencies of choice of the right number of blocks, i.e.,  $\hat{Q}_1 = \hat{Q}_2 = 4$ . As one can see, the structure is not recovered for small values of  $\epsilon_\alpha$ , which is not surprising since in this case, the network is close to an Erdős-Rényi model. However, as soon as  $\epsilon_\alpha$  is over 0.06 the methods recovers the true numbers of blocks in most cases (frequency higher than 0.61). Even more remarkably, the 4 – 4 block structure is also found in the majority of cases, even if the assumption on the proportions is not the right one (columns 1, 2, and 3 of the table).

To go further, we evaluate the quality of the clustering of the nodes into the blocks depending on the chosen model. To compare the inferred clustering (denote  $\hat{\mathbf{Z}}$ ) with the simulated/true ones (denote  $\mathbf{Z}^*$ ), we use the Adjusted Rand Index (ARI, [Hubert and Arabie, 1985](#)) which is a measure of the similarity between two clusterings:  $ARI = 0$  for a random clustering while  $ARI = 1$  for a perfect match between clusterings<sup>1</sup>. For each network, we compare the block memberships obtained respectively by the  $\pi$ -colBiSBM,  $\rho$ -colBiSBM and  $\pi\rho$ -colBiSBM models to the true ones. To do so, we compute the mean of the ARI per dimension (rows and cols) over the 2 networks:

$$\begin{aligned}\overline{ARI}_{row} &= \frac{1}{2} \left[ ARI(\hat{\mathbf{Z}}^1, \mathbf{Z}^{*1}) + ARI(\hat{\mathbf{Z}}^2, \mathbf{Z}^{*2}) \right], \\ \overline{ARI}_{col} &= \frac{1}{2} \left[ ARI(\hat{\mathbf{W}}^1, \mathbf{W}^{*1}) + ARI(\hat{\mathbf{W}}^2, \mathbf{W}^{*2}) \right].\end{aligned}$$

The evolutions of  $\overline{ARI}_{row}$  and  $\overline{ARI}_{col}$  as  $\epsilon_\alpha$  increases are plotted on the top line of Figure S-2. As we see, the intra network clustering of the nodes is very good for every model as soon as  $\epsilon_\alpha$  exceeds 0.09. However, we have to check if the blocks are coherent from one network to another: i.e., we want to be sure the block  $k$  of network 1 indeed corresponds to block  $k$  in network 2. To do so, we concatenate the row node clustering ( $\mathbf{Z}^1, \mathbf{Z}^2$ ) and compute the global ARI (across networks) in row and col as:

$$\begin{aligned}ARI_{row} &= ARI((\hat{\mathbf{Z}}^1, \hat{\mathbf{Z}}^2), (\mathbf{Z}^{*1}, \mathbf{Z}^{*2})) \\ ARI_{col} &= ARI((\hat{\mathbf{W}}^1, \hat{\mathbf{W}}^2), (\mathbf{W}^{*1}, \mathbf{W}^{*2}))\end{aligned}$$

The evolutions of  $ARI_{row}$  and  $ARI_{col}$  as  $\epsilon_\alpha$  increases are plotted in the bottom line of Figure S-2. As expected, the global ARI of the sep-colBiSBM is around  $\frac{1}{2}$ . Indeed, in this case, no coherence between the networks is introduced and consequently, due to label switching, the blocks are randomly matched leading to the observed phenomena. When  $\epsilon_\alpha$  increases the global ARI for iid-colBiSBM and  $\pi\rho$ -colBiSBM stabilizes around 0.9: the proposed colBiSBM are able to recover the common structure in the 2 networks and gather nodes from various networks playing the same role. For  $\pi$ -colBiSBM and  $\rho$ -colBiSBM the stabilization occurs around 0.7 and 0.8, the differences with the best models can be interpreted as the need of either having no flexibility or complete flexibility on both axis to not hinder performances by introducing some possible confusion.

---

<sup>1</sup>Note that even if Rand Index can only yield values between 0 and 1, ARI can return negative values if the RI is less than the expected value. This indicates a structure in clustering discordance.

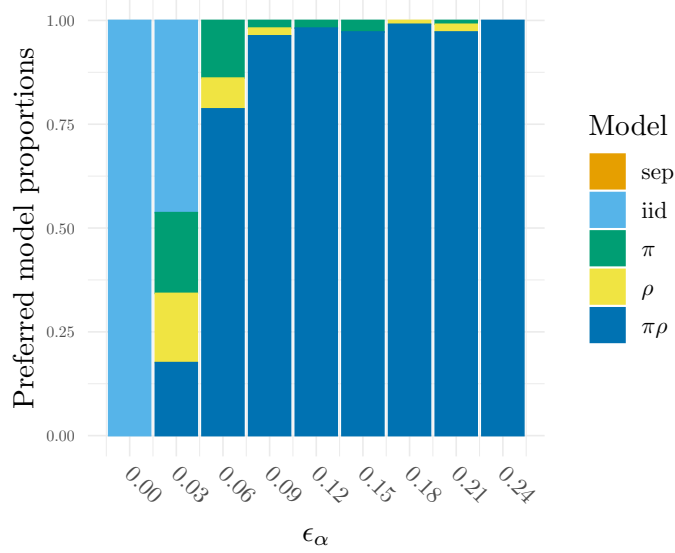


Figure S-1 – *Assessing the quality of estimation*: Preferred model proportions over all datasets in function of  $\epsilon_\alpha$

Table S-1 – *Assessing the quality of estimation*: proportion of datasets where the correct numbers of blocks are selected.

$\epsilon_\alpha$	iid-colBiSBM		$\pi$ -colBiSBM		$\rho$ -colBiSBM		$\pi\rho$ -colBiSBM	
	$\mathbf{1}_{\widehat{Q}_1=4}$	$\mathbf{1}_{\widehat{Q}_2=4}$	$\mathbf{1}_{\widehat{Q}_1=4}$	$\mathbf{1}_{\widehat{Q}_2=4}$	$\mathbf{1}_{\widehat{Q}_1=4}$	$\mathbf{1}_{\widehat{Q}_2=4}$	$\mathbf{1}_{\widehat{Q}_1=4}$	$\mathbf{1}_{\widehat{Q}_2=4}$
0.00	0	0	0	0	0	0	0	0
0.03	0	0	0	0	0	0	0	0
0.06	$0.64 \pm 0.05$	$0.61 \pm 0.05$	$0.67 \pm 0.05$	$0.64 \pm 0.05$	$0.66 \pm 0.05$	$0.59 \pm 0.05$	$0.86 \pm 0.03$	$0.86 \pm 0.03$
0.09	$0.97 \pm 0.02$	$0.94 \pm 0.02$	$0.71 \pm 0.04$	1	1	$0.64 \pm 0.05$	$0.83 \pm 0.04$	$0.88 \pm 0.03$
0.12	$0.91 \pm 0.03$	$0.91 \pm 0.03$	$0.74 \pm 0.04$	1	1	$0.66 \pm 0.05$	$0.92 \pm 0.03$	$0.91 \pm 0.03$
0.15	$0.91 \pm 0.03$	$0.94 \pm 0.02$	$0.83 \pm 0.04$	1	1	$0.71 \pm 0.04$	$0.92 \pm 0.03$	$0.94 \pm 0.02$
0.18	$0.93 \pm 0.03$	$0.89 \pm 0.03$	$0.81 \pm 0.04$	1	1	$0.73 \pm 0.04$	$0.94 \pm 0.02$	$0.94 \pm 0.02$
0.21	$0.91 \pm 0.03$	$0.92 \pm 0.03$	$0.83 \pm 0.04$	1	1	$0.7 \pm 0.04$	$0.88 \pm 0.03$	$0.9 \pm 0.03$
0.24	$0.9 \pm 0.03$	$0.92 \pm 0.03$	$0.81 \pm 0.04$	1	1	$0.79 \pm 0.04$	$0.93 \pm 0.03$	$0.93 \pm 0.03$

## D.2 From fixed to varying block proportions

In this numerical experiment, we test our capacity to distinguish  $\pi\rho$ -colBiSBM from iid-colBiSBM and other models

**Simulation settings** To do so, we simulate  $M = 3$  networks of the same size involving  $n_1^m = 90$  row nodes and  $n_2^m = 90$  column nodes. We fix a connection structure

$$\alpha = \begin{pmatrix} 0.73 & 0.57 & 0.41 \\ 0.57 & 0.57 & 0.09 \\ 0.41 & 0.09 & 0.41 \end{pmatrix}.$$

We vary the difficulty to decipher between the models by setting the block proportions as follows:

$$\begin{aligned} \pi^1 &= \left(\frac{1}{3}, \frac{1}{3}, \frac{1}{3}\right), & \rho^1 &= \left(\frac{1}{3}, \frac{1}{3}, \frac{1}{3}\right), \\ \pi^2 &= \sigma\left(\frac{1}{3} - \epsilon_\pi, \frac{1}{3}, \frac{1}{3} + \epsilon_\pi\right), & \rho^2 &= \sigma\left(\frac{1}{3} - \epsilon_\rho, \frac{1}{3}, \frac{1}{3} + \epsilon_\rho\right), \\ \pi^3 &= \sigma\left(\frac{1}{3} + \epsilon_\pi, \frac{1}{3}, \frac{1}{3} - \epsilon_\pi\right), & \rho^3 &= \sigma\left(\frac{1}{3} + \epsilon_\rho, \frac{1}{3}, \frac{1}{3} - \epsilon_\rho\right), \end{aligned}$$

where  $\epsilon_\pi$  and  $\epsilon_\rho$  takes 9 values equally spaced in  $[0, 0.28]$ . For each combination of parameters,  $N = 3$  repetitions are conducted. Note that when  $\epsilon_\pi = 0$  and  $\epsilon_\rho = 0$ , the true model is the

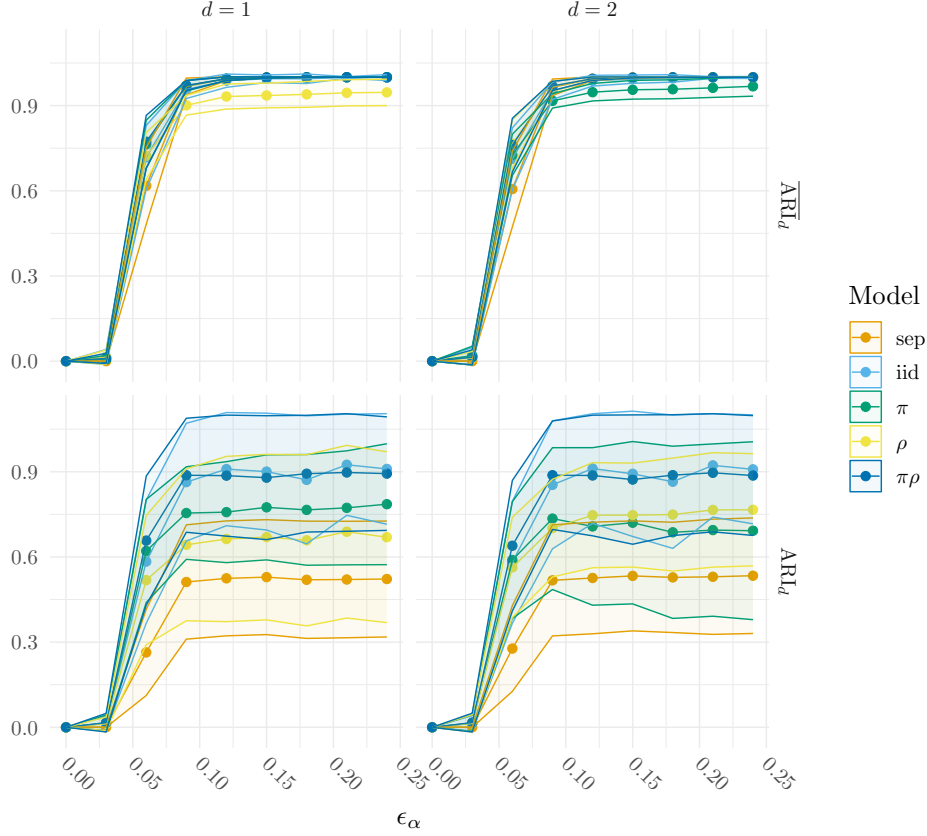


Figure S-2 – *Assessing the quality of estimation*: Plot of the ARI quality indicators in function of  $\epsilon_\alpha$

iid-colBiSBM. When  $\epsilon_\pi > 0$  and  $\epsilon_\rho = 0$  the true model is a  $\pi$ -colBiSBM. When  $\epsilon_\pi = 0$  and  $\epsilon_\rho > 0$  the true model is a  $\rho$ -colBiSBM. Finally, when  $\epsilon_\pi > 0$  and  $\epsilon_\rho > 0$ , the true model is a  $\pi\rho$ -colBiSBM. The five models  $\pi\rho$ -colBiSBM,  $\pi$ -colBiSBM,  $\rho$ -colBiSBM, iid-colBiSBM and  $\text{sep}$ -colBiSBM are fitted, and the preferred model is chosen by the BIC-L criterion.

**Results** Figure S-3 shows the selection frequency of each model across simulations. As expected, the  $\text{sep}$ -colBiSBM is never selected. When  $\epsilon_\pi$  or  $\epsilon_\rho$  is close to 0, the iid-colBiSBM model is predominantly selected. A noticeable transition occurs around  $\epsilon_\pi = 0.14$ , marking a shift in the preferred models. Before this threshold, the iid-colBiSBM and the  $\rho$ -colBiSBM are frequently selected. Beyond this point, the  $\pi$ -colBiSBM and  $\pi\rho$ -colBiSBM are increasingly favored. A similar result is observed on the other axis around  $\epsilon_\rho = 0.14$  favoring the  $\rho$ -colBiSBM and  $\pi\rho$ -colBiSBM after this threshold. Eventually, when the group proportions differ significantly across networks, the  $\pi\rho$ -colBiSBM is systematically selected. The fact that both  $\epsilon_\pi$  and  $\epsilon_\rho$  need to exceed 0.17 before the  $\pi\rho$  model is preferred suggests that a strong inter-network difference is required to justify selecting this model. The below Table S-2 shows the retrieval percentage of the correct number of blocks in the model selection experiment presented in Section 4.4.

The proportions of correct block number selected stay relatively high for all models and  $\epsilon_\pi, \epsilon_\rho$  but something interesting can be seen for the  $\pi$ -colBiSBM and  $\rho$ -colBiSBM. When the other axis e.g., the columns for the  $\pi$ -colBiSBM sees the proportions differences increased it diminishes the correct retrieval rate for the free axis. One may suspect other causes but the performance of the  $\pi\rho$ -colBiSBM being near perfect invites us to point in the direction of a confusion induced in the free axis by the non-free one.

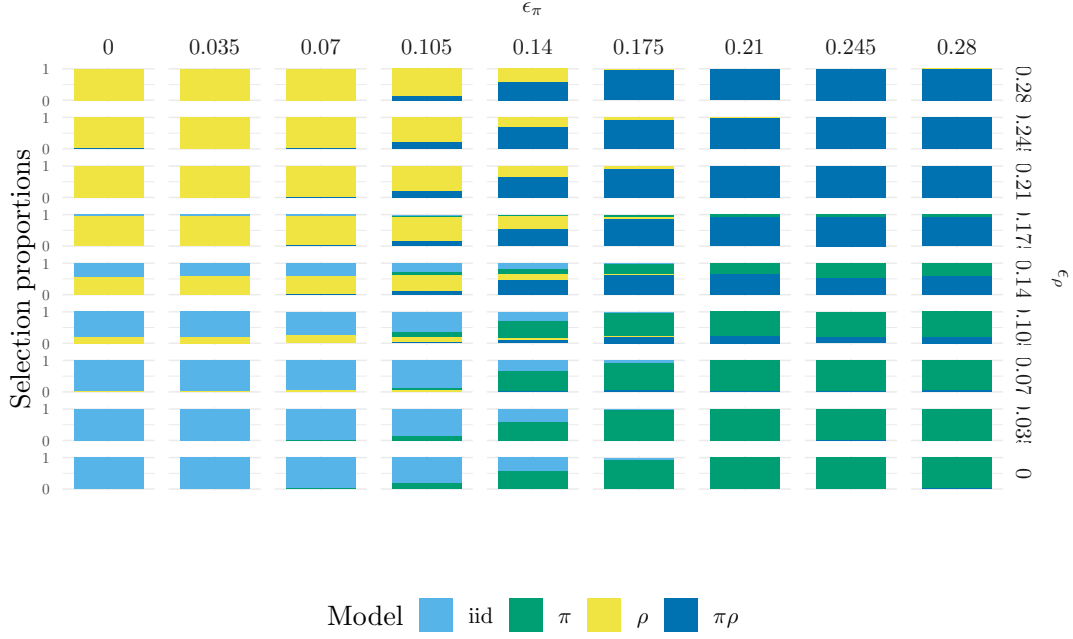


Figure S-3 – *From fixed to varying block proportions*: Plot of model selection proportions over the different datasets in function of  $\epsilon_\pi$  and  $\epsilon_\rho$

Table S-2 – *From fixed to varying block proportions*. Proportion of dataset where the correct number of blocks is selected. Only shows results for  $\epsilon_\rho \in \{0, 0.14, 0.28\}$ .

$\epsilon_\pi$	$\epsilon_\rho$	iid		$\pi$		$\rho$		$\pi\rho$	
		$\mathbf{1}_{\widehat{Q}_{1iid}=3}$	$\mathbf{1}_{\widehat{Q}_{2iid}=3}$	$\mathbf{1}_{\widehat{Q}_{1\pi}=3}$	$\mathbf{1}_{\widehat{Q}_{2\pi}=3}$	$\mathbf{1}_{\widehat{Q}_{1\rho}=3}$	$\mathbf{1}_{\widehat{Q}_{2\rho}=3}$	$\mathbf{1}_{\widehat{Q}_{1\pi\rho}=3}$	$\mathbf{1}_{\widehat{Q}_{2\pi\rho}=3}$
0.000	0.00	1	1	1	1	1	1	1	1
0.000	0.14	$0.99 \pm 0.01$	1	1	1	1	1	1	1
0.000	0.28	$0.93 \pm 0.03$	$0.99 \pm 0.01$	$0.81 \pm 0.04$	1	1	1	1	1
0.035	0.00	1	1	1	1	1	1	1	1
0.035	0.14	1	1	1	1	1	1	1	1
0.035	0.28	$0.97 \pm 0.02$	$0.96 \pm 0.02$	$0.86 \pm 0.03$	1	1	1	1	1
0.070	0.00	1	1	1	1	1	1	1	1
0.070	0.14	1	1	1	1	1	1	$0.99 \pm 0.01$	1
0.070	0.28	$0.95 \pm 0.02$	$0.96 \pm 0.02$	$0.78 \pm 0.04$	1	1	1	$0.99 \pm 0.01$	$0.99 \pm 0.01$
0.105	0.00	1	1	1	1	1	1	1	1
0.105	0.14	1	1	1	1	1	1	1	1
0.105	0.28	$0.96 \pm 0.02$	$0.95 \pm 0.02$	$0.79 \pm 0.04$	1	1	1	$0.99 \pm 0.01$	$0.99 \pm 0.01$
0.140	0.00	1	1	1	1	1	1	1	1
0.140	0.14	$0.98 \pm 0.01$	$0.99 \pm 0.01$	1	1	1	1	1	1
0.140	0.28	$0.98 \pm 0.01$	$0.94 \pm 0.02$	$0.81 \pm 0.04$	1	1	$0.99 \pm 0.01$	$0.99 \pm 0.01$	1
0.175	0.00	1	1	1	1	1	1	1	1
0.175	0.14	$0.98 \pm 0.01$	$0.98 \pm 0.01$	$0.99 \pm 0.01$	1	1	$0.99 \pm 0.01$	1	1
0.175	0.28	$0.98 \pm 0.01$	$0.97 \pm 0.02$	$0.82 \pm 0.04$	1	1	1	1	1
0.210	0.00	$0.99 \pm 0.01$	$0.98 \pm 0.01$	1	1	1	$0.99 \pm 0.01$	1	1
0.210	0.14	$0.99 \pm 0.01$	$0.96 \pm 0.02$	$0.99 \pm 0.01$	1	1	$0.99 \pm 0.01$	1	1
0.210	0.28	$0.94 \pm 0.02$	$0.95 \pm 0.02$	$0.75 \pm 0.04$	1	1	$0.98 \pm 0.01$	$0.99 \pm 0.01$	$0.99 \pm 0.01$
0.245	0.00	$0.99 \pm 0.01$	$0.97 \pm 0.02$	1	1	1	$0.97 \pm 0.02$	1	1
0.245	0.14	$0.94 \pm 0.02$	$0.95 \pm 0.02$	$0.99 \pm 0.01$	1	1	$0.98 \pm 0.01$	1	1
0.245	0.28	$0.94 \pm 0.02$	$0.93 \pm 0.03$	$0.72 \pm 0.04$	1	1	$0.94 \pm 0.02$	1	1
0.280	0.00	$0.98 \pm 0.01$	$0.92 \pm 0.03$	$0.99 \pm 0.01$	1	1	$0.86 \pm 0.03$	1	1
0.280	0.14	$0.96 \pm 0.02$	$0.95 \pm 0.02$	$0.98 \pm 0.01$	1	1	$0.86 \pm 0.03$	1	1
0.280	0.28	$0.94 \pm 0.02$	$0.96 \pm 0.02$	$0.77 \pm 0.04$	1	1	$0.73 \pm 0.04$	$0.99 \pm 0.01$	$0.98 \pm 0.01$

### D.3 Information transfer between networks

One of the motivations for modeling collections of networks jointly rather than separately is the potential for *information transfer* between them. To illustrate this advantage, we evaluate how information can be transferred from a large network to a smaller one with missing values, aiming to recover the fine structure of the smaller network. In particular, we compare the performance of different methods in retrieving the node blocks affected by missing edges.

#### D.3.1 On modular structure

**Simulation settings** For this purpose we generate collections with two networks ( $M = 2$ ) of size  $n_1^1 = n_2^1 = 20$  and  $n_1^2 = n_2^2 = 120$ . One collection is generated for each colBiSBM model. For each colBiSBM model, the experiment is repeated  $N = 10$  times.

$$\pi^m = \begin{cases} \pi = (0.5, 0.3, 0.2) & \text{for iid} \\ \sigma_1^m(\pi) & \text{for } \pi \text{ and } \pi\rho \end{cases}, \quad \rho^m = \begin{cases} \rho = (0.5, 0.3, 0.2) & \text{for iid} \\ \sigma_2^m(\rho) & \text{for } \rho \text{ and } \pi\rho \end{cases},$$

for the block proportions, and two different structures with the corresponding  $\alpha$ ,

$$\alpha^{modular} = \begin{pmatrix} 0.9 & 0.05 & 0.05 \\ 0.05 & 0.2 & 0.05 \\ 0.05 & 0.05 & 0.8 \end{pmatrix}$$

where  $\alpha^{modular}$  represents networks with community structure, i.e., pairs of blocks that tend to interact preferentially within the block and less outside of the blocks. In network  $m = 1$  (i.e., the smallest one) a proportion of the edges  $p_{\text{mis}}$  see their values replaced by NAs.

**Test procedure** A standard biSBM is fitted on the first network alone, and the predicted block memberships are saved, along with the predicted links using the inferred parameters. This will serve as a baseline to see if the use of the collection benefits the predictions. A colBiSBM model is then fitted of the two networks and we store the then obtained predictions of the missing links of network  $m = 1$ .

**Quality metrics** To benchmark the performance we use the *ROC Area Under the Curve* (ROC AUC) for predicted versus real link values and the ARI that compare the predicted block memberships to the true block memberships.



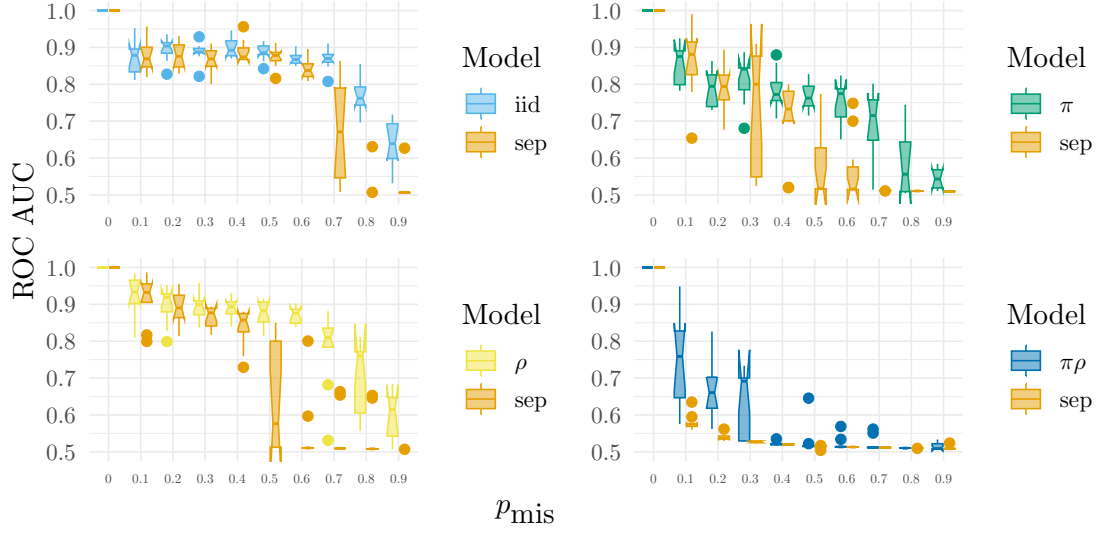


Figure S-4 – *Information transfer on modular structure*: ARI over rows and columns in function of  $p_{\text{mis}}$ , the proportion of missing links for the four colBiSBM models and their LBM counterparts. Each dataset is generated with the corresponding colBiSBM model on a modular structure and fitted with the same model and the LBM model labelled as sep-colBiSBM to give a baseline of the performance.

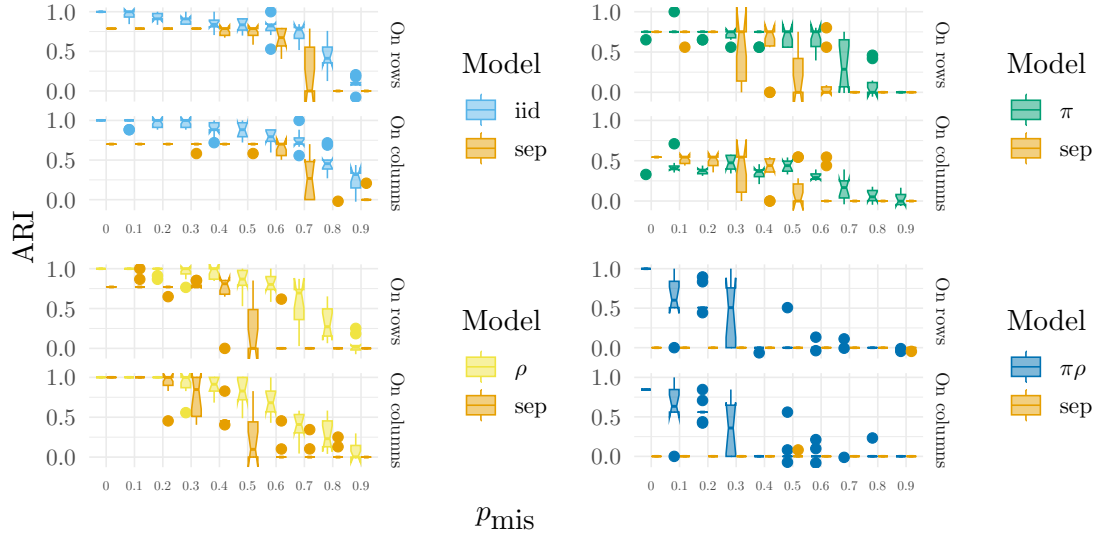


Figure S-5 – *Information transfer on modular structure*: AUC over rows and columns in function of  $p_{\text{mis}}$ , the proportion of missing links for the four colBiSBM models and their LBM counterparts. Each dataset is generated with the corresponding colBiSBM model on a modular structure and fitted with the same model and the LBM model labelled as sep-colBiSBM to give a baseline of the performance.

**Results** Figures S-4 and S-5 show the results for the colBiSBM model and its sep-biSBM counterpart fitted on the same data.

For the AUC (Figure S-4), in almost all cases and for almost all models the differences are not significant, but our models seem to perform marginally better than their LBM counterpart and with a smaller variance. The colBiSBM models seem able to endure higher degradation levels than the sep counterpart. This indicates that information is transferred from the bigger network that can learn the full structure when estimating the parameters and predicting link

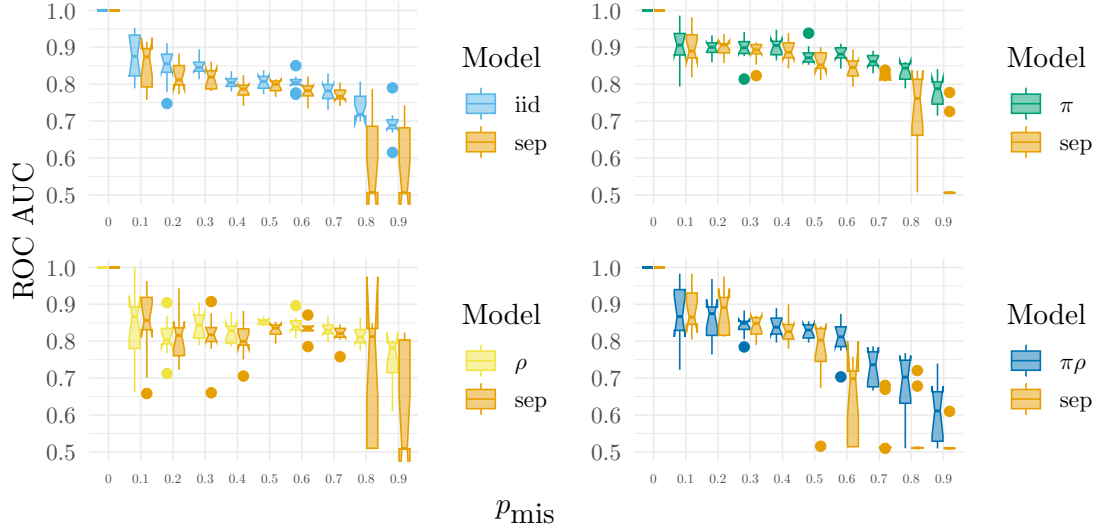


Figure S-6 – *Information transfer on nested structure*: ROC AUC in function of  $p_{\text{mis}}$ , the proportion of missing links for the four colBiSBM models and their LBM counterparts. Each dataset is generated with the corresponding colBiSBM model on a nested structure and fitted with the same model and the LBM model labelled as sep to give a baseline of the performance.

values.

For the ARI (Figure S-5), our models almost always do at least as good as the sep counterpart and with a smaller variance. The block membership attribution for rows for  $\pi$ -colBiSBM reveals more challenging and yields an ARI of at most 0.75. And for the  $\pi\rho$  datasets the sep is completely random (ARI = 0) and the  $\pi\rho$ -colBiSBM is only better for the very low proportions of missing data.

### D.3.2 Simulation on nested structure

**Simulation settings** We use the same simulation settings, test procedure and quality metrics as in Section D.3. The only difference being the connectivity structure,

$$\boldsymbol{\alpha}^{\text{nested}} = \begin{pmatrix} 0.9 & 0.65 & 0.1 \\ 0.35 & 0.15 & 0.05 \\ 0.1 & 0.05 & 0.05 \end{pmatrix}$$

where  $\boldsymbol{\alpha}^{\text{nested}}$  represents a common structure detected in ecology with generalist and specialist species and a “nested” structure.

**Results** Figures S-6 and S-7 respectively present the results of the simulation for AUC and ARI metrics.

From Figure S-6 we see result similar to Figure S-4, our models always perform at least as best as the baseline sep and with smaller variability. But the performance difference is marginal and non significant except in very degraded case ( $p_{\text{mis}} \geq 0.7$ ).

On Figure S-7, we see trends similar to Section D.3.1. All models at worst equal their sep counterpart (apart from iid for rows at  $p_{\text{mis}} = 0.6$ ). For the iid and  $\rho$  datasets the sep is having trouble on columns and rows respectively.

Four main differences from Section D.3.1 are that iid-colBiSBM gives poor performance node membership attribution for columns, for  $\rho$ -colBiSBM on rows it performs a bit better than the sep but not exceeding 0.5, still for  $\rho$ -colBiSBM on columns the ARI is at 1 until a sudden

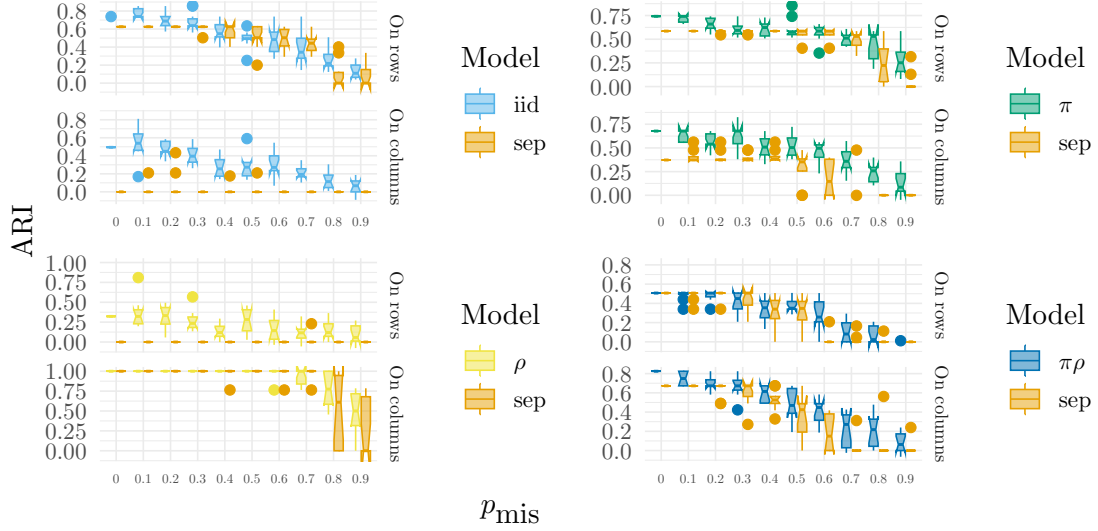


Figure S-7 – *Information transfer on nested structure*: ARI over rows and columns in function of  $p_{\text{mis}}$ , the proportion of missing links for the four colBiSBM models and their LBM counterparts. Each dataset is generated with the corresponding colBiSBM model on a nested structure and fitted with the same model and the LBM model labelled as sep to give a baseline of the performance.

variability increase and drop around  $p_{\text{mis}} \geq 0.8$  and the  $\pi\rho$ -colBiSBM is less drastically bad around 0.55 slowly decreasing to 0.1 but still beating the sep.

What we learn from Sections D.3.1 and D.3.2 is twofold. The structure of connectivity of the networks can drastically change the performance of the inference algorithm. We see that nested structures resist to higher levels of degradation than modular structures. In the end the joint modeling still benefits from the information transfer it allows even in harder settings.

## D.4 Clustering of simulated networks

**Simulation settings** For all models we simulate  $M = 30$  networks with  $\forall m \in \{1 \dots M\}, n_1^m = n_2^m = 75$  with  $Q_1 = Q_2 = 3$ .

For the simulations the proportions are the following:

$\pi^1 = (0.2, 0.3, 0.5)$ ,  $\rho^1 = (0.2, 0.3, 0.5)$  and for all  $m = 2, \dots, 9$

$$\pi^m = \begin{cases} \pi^1 & \text{for iid} \\ \sigma_1^m(\pi^1) & \text{for } \pi \text{ and } \pi\rho \end{cases}, \quad \rho^m = \begin{cases} \rho^1 & \text{for iid} \\ \sigma_2^m(\rho^1) & \text{for } \rho \text{ and } \pi\rho \end{cases},$$

where  $\sigma_1^m$  and  $\sigma_2^m$  are permutations of  $\{1, 2, 3\}$  proper to network  $m$  and  $\sigma_1(\pi) = (\pi_{\sigma_1(i)})_{i=\{1, \dots, 3\}}$  and  $\sigma_2(\rho) = (\rho_{\sigma_2(i)})_{i=\{1, \dots, 3\}}$ .

The networks are divided into 3 sub-collections of 10 networks with connectivity parameters as follows:

$$\alpha^{as} = .3 + \begin{pmatrix} \epsilon & -\frac{\epsilon}{2} & -\frac{\epsilon}{2} \\ -\frac{\epsilon}{2} & \epsilon & -\frac{\epsilon}{2} \\ -\frac{\epsilon}{2} & -\frac{\epsilon}{2} & \epsilon \end{pmatrix}, \quad \alpha^{dis} = .3 + \begin{pmatrix} -\frac{\epsilon}{2} & \epsilon & \epsilon \\ \epsilon & -\frac{\epsilon}{2} & \epsilon \\ \epsilon & \epsilon & -\frac{\epsilon}{2} \end{pmatrix}, \quad \alpha^{cp} = .3 + \begin{pmatrix} \frac{3\epsilon}{2} & \epsilon & \frac{\epsilon}{2} \\ \epsilon & \frac{\epsilon}{2} & 0 \\ \frac{\epsilon}{2} & 0 & -\frac{\epsilon}{2} \end{pmatrix}$$

with  $\epsilon \in [.1, .4]$ .  $\alpha^{as}$  represents a classical assortative community structure, while  $\alpha^{cp}$  is a layered core-periphery structure with block 2 acting as a semi-core. Finally,  $\alpha^{dis}$  is a disassortative community structure with stronger connections between blocks than within blocks.

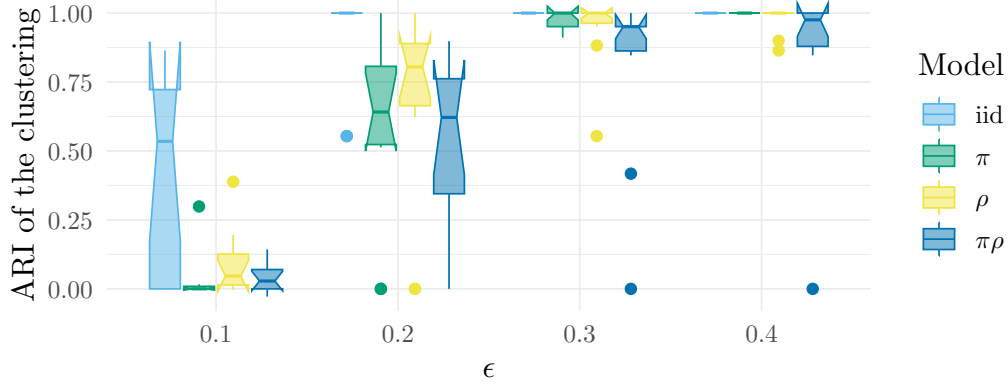


Figure S-8 – ARI obtained for the partitioning with the different models in function of  $\epsilon$

If  $\epsilon = 0$ , the three matrices are equal and the 9 networks have the same connection structure thus making the node membership attribution and partitioning of the different structure types difficult. Increasing  $\epsilon$  differentiates the 3 sub-collections of networks and makes the classification task easier.

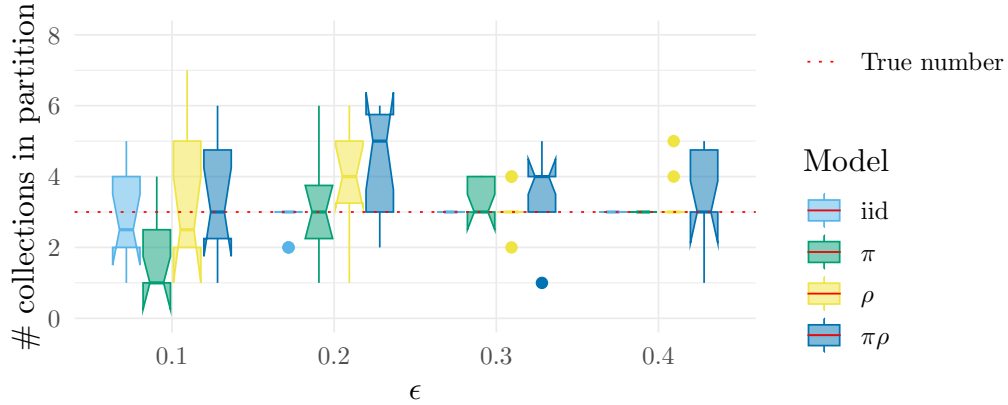


Figure S-9 – Number of collections in partition obtained for the clustering with the different models in function of  $\epsilon$ . The true number of collections is 3 plotted by the red dashed line.

**Results** The evaluation of our method involves a comparison between the resulting partition of the network collection and the simulated partition using the ARI metric (Figure S-8). As the value of  $\epsilon$  increases, our ability to distinguish between the networks improves, and this distinction becomes nearly perfect in all setups of the colBiSBM as soon as  $\epsilon \geq 0.3$ .

The number of collections in the partition obtained for the clustering with the different models is plotted in Figure S-9. There is a variation in the number of collections yielded by the algorithm for the iid,  $\pi$  and  $\rho$  models the medians settle around true value for  $\epsilon_\alpha \geq 0.3$  while for the  $\pi\rho$  it happens for  $\epsilon_\alpha = 0.4$ . This may be due to the fact that there is more freedom in the  $\pi\rho$  model and thus more variability. Looking at the number of partition helps understand why some partitioning yields an ARI of 0, this is due to the partitioning algorithm deciding to stop after fitting the full collection and not proposing any cut.

## E Data for applications on ecological networks

Table S-3 – Shared species over total species for both pollinators and plants for the 5 Baldock networks.

	TB+JN	Bristol	Edinburgh	Leeds	Reading
TB+JN					
Bristol	$\frac{0}{237}, \frac{1}{301}$				
Edinburgh	$\frac{0}{181}, \frac{1}{250}$	$\frac{73}{257}, \frac{73}{236}$			
Leeds	$\frac{0}{198}, \frac{1}{247}$	$\frac{76}{271}, \frac{79}{227}$	$\frac{61}{230}, \frac{58}{197}$		
Reading	$\frac{0}{200}, \frac{1}{288}$	$\frac{73}{276}, \frac{89}{258}$	$\frac{66}{227}, \frac{62}{234}$	$\frac{69}{241}, \frac{74}{219}$	